

BASIC-ALIMENTARY TRACT

Figure 1. Association of the SNPs around rs2070803 and rs2075570 in chromosome 1q22 with GC and LD analyses of the SNPs. (A) The association study on DGC disclosed 8 SNPs with $P < 4 \times 10^{-5}$ within the LD block around rs2070803 and rs2075570 (arrows in B) in the Japanese population (Tokyo data set: blue dots). The association with DGC was replicated in another Japanese population (Aichi data set: orange dots) and also in the Korean population (Korea data set: red dots) for 4 selected SNPs: rs2070803, rs4072037, rs2066981, and rs2075570 ($P < 1 \times 10^{-3}$). Meta-analysis on these 3 data sets was also conducted (Tokyo and Aichi: grey dots; Tokyo, Aichi, and Korea: black dots). The study on IGC in the Japanese population (Tokyo data set: 599 cases, 1264 controls) showed no significant association of SNPs (green dots). Upper panel shows P value of each SNP in negative logarithmic scale; lower panel shows OR and frequency of the risk allele (control RAF) of the SNPs. The position of the dots representing each SNP corresponds vertically to that in the physical map in B. (B) An LD analysis based on $|D'|$ showed a strong LD around the 2 SNPs, rs2070803 and rs2075570 (red arrows), identified as DGC-associated SNPs in GWAS.⁷ The strength of the LD is indicated by heat maps. Blue bars represent LD blocks defined by confidence intervals of $|D'|$.¹⁵ Five genes—KRTCAP2, TRIM46, MUC1, THBS3, and MTX1—reside in the region of strong LD (double-headed red arrow) harboring rs2070803 and rs2075570. An LD map with r^2 is also shown in small scale. The analysis was performed with genotyping data of 1266 controls of the Tokyo data set.

of Association Studies With 3 Independent Data Sets—Tokyo, Aichi, and Korea—for GC Susceptibility, on the 8 SNPs in the LD Block Containing rs103 and rs2075570 in Chromosome 1q22

Diffuse, Tokyo data set ^{a,c}	Diffuse, Aichi data set ^{a,d}	Diffuse, Korea data set ^{a,e}	Diffuse, Meta-analysis ^{a,f}	Diffuse, Meta-analysis ^{a,h}	Intestinal, Tokyo data set ^{a,i}
OR: 1.61 (1.32–1.97) P: 3.17×10^{-6} MAF (case): 0.133 MAF (control): 0.199					OR: 1.22 (1.01–1.43) P: 3.62×10^{-5} MAF (case): 0.103 MAF (control): 0.164
OR: 1.63 (1.33–1.99) P: 2.04×10^{-6} MAF (case): 0.133 MAF (control): 0.200					OR: 1.22 (1.02–1.42) P: 3.13×10^{-5} MAF (case): 0.103 MAF (control): 0.164
OR: 1.63 (1.33–1.99) P: 2.20×10^{-6} MAF (case): 0.133 MAF (control): 0.200	OR: 1.81 (1.36–2.40) P: 3.93×10^{-5} MAF (case): 0.104 MAF (control): 0.178	OR: 1.82 (1.32–2.49) P: 2.19×10^{-4} MAF (case): 0.103 MAF (control): 0.178	OR: 1.69 (1.43–1.99) P: 4.25×10^{-10}	OR: 1.71 (1.48–1.98) P: 4.33×10^{-13}	OR: 1.22 (1.02–1.42) P: 3.34×10^{-5} MAF (case): 0.103 MAF (control): 0.164
OR: 1.62 (1.32–1.99) P: 4.04×10^{-6} MAF (case): 0.126 MAF (control): 0.187	OR: 1.69 (1.27–2.25) P: 2.82×10^{-4} MAF (case): 0.099 MAF (control): 0.164	OR: 1.74 (1.26–2.39) P: 7.82×10^{-4} MAF (case): 0.093 MAF (control): 0.163	OR: 1.64 (1.39–1.94) P: 4.46×10^{-9}	OR: 1.66 (1.44–1.93) P: 1.43×10^{-11}	OR: 1.23 (1.02–1.43) P: 3.36×10^{-5} MAF (case): 0.103 MAF (control): 0.164
OR: 1.61 (1.31–1.98) P: 5.91×10^{-6} MAF (case): 0.125 MAF (control): 0.186	OR: 1.74 (1.31–2.32) P: 1.50×10^{-4} MAF (case): 0.099 MAF (control): 0.167	OR: 1.76 (1.27–2.43) P: 6.98×10^{-4} MAF (case): 0.092 MAF (control): 0.159	OR: 1.65 (1.40–1.95) P: 3.77×10^{-9}	OR: 1.67 (1.44–1.94) P: 1.11×10^{-11}	OR: 1.21 (1.01–1.41) P: 4.41×10^{-5} MAF (case): 0.103 MAF (control): 0.164
OR: 1.61 (1.31–1.98) P: 5.83×10^{-6} MAF (case): 0.126 MAF (control): 0.187					OR: 1.22 (1.01–1.43) P: 3.94×10^{-5} MAF (case): 0.103 MAF (control): 0.164
OR: 1.63 (1.32–2.00) P: 3.45×10^{-6} MAF (case): 0.127 MAF (control): 0.189	OR: 1.77 (1.33–2.37) P: 1.12×10^{-4} MAF (case): 0.100 MAF (control): 0.170	OR: 1.84 (1.32–2.55) P: 2.73×10^{-4} MAF (case): 0.091 MAF (control): 0.163	OR: 1.67 (1.42–1.98) P: 1.73×10^{-9}	OR: 1.71 (1.47–1.98) P: 2.26×10^{-12}	OR: 1.21 (1.01–1.41) P: 4.25×10^{-5} MAF (case): 0.103 MAF (control): 0.164
OR: 1.67 (1.36–2.04) P: 6.59×10^{-7} MAF (case): 0.130 MAF (control): 0.200					OR: 1.25 (1.04–1.46) P: 1.95×10^{-5} MAF (case): 0.103 MAF (control): 0.164

OR, Odds ratio for risk allele with 95% confidence intervals in parentheses.

SNP, single nucleotide polymorphism.

MAF, minor allele frequency; alleles are common in Tokyo, Aichi, and Korea data sets.

Diffuse-type GC in the Japanese population (Tokyo data set: 606 cases, 1264 controls), performed with fine-mapping data.

95% CI were calculated under an additive model using logistic regression adjusted for age, gender, and number of risk alleles of rs2294008 of the PSCA gene, which was associated with diffuse-type GC in the Japanese population (Tokyo data set: 606 cases, 1264 controls), performed with fine-mapping data.

Diffuse-type GC in the Japanese population (Aichi data set: 304 cases, 1465 controls), for replication of the study on Tokyo data set.

Diffuse-type GC in the Korean population (Korea data set: 452 cases, 372 controls), for replication of the study on Tokyo data set.

MAF, minor allele frequency; alleles are common in the Tokyo and Aichi data sets.

95% CI were calculated using a random effects model.

MAF, minor allele frequency; alleles are common in the Tokyo, Aichi, and Korea data sets.

Intestinal-type GC in the Japanese population (Tokyo data set: 599 cases, 1264 controls).

MAF, minor allele frequency; alleles are common in the Tokyo, Aichi, and Korea data sets.

BASIC-
ALIMENTARY TRACT

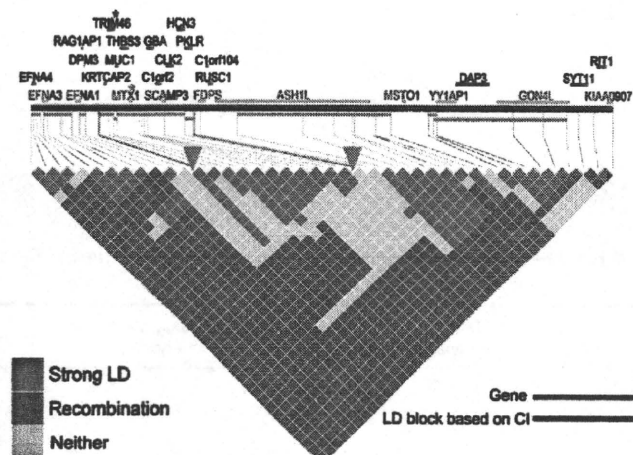


Figure 2. LD analyses on the SNPs in chromosome 1q22 using Gabriel's criteria¹⁵ based on genotyping data of 680 Japanese controls. LD blocks with the criteria are in blue horizontal lines. Red asterisks indicate positions of rs2075570 and rs2070803. The LD block (both ends indicated by red triangles), in which the 2 SNPs reside, contains 12 SNPs and 11 genes. CI, confidence interval.

56.1; 178 females; mean age, 54.6; 2 missing gender information; 372 of which were the same as DGC cases in the Tokyo data set) and 309 controls (151 males; mean age, 49.1; 158 females; mean age, 46.1; 306 of which were included in the Tokyo data set). DGC samples were collected at 2 institutions as follows: 318 paraffin-embedded tissues at the National Cancer Center Hospital, and 62 blood samples at Nippon Medical School Hospital. Control DNA samples were from Keio University campuses.

The Japanese part of the study was approved by the ethics committees of the participating institutions in accordance with the Ethics Guidelines For Human Genome/Gene Analysis Research in Japan. The Korean side of the GC case control study was approved by the Ethics Committee of the National Cancer Center, Korea. Informed consent was obtained from all living subjects, including opt-out consent for the paraffin block archival samples.

LD Analysis

The LD map of chromosome 1q22 (Figure 2) was constructed based on the genotype data of 41 SNPs (Supplementary Table 10) obtained from 680 Japanese controls (436 males; mean age, 43.7; 242 females; mean age, 43.7; 2 missing gender information; 371 of which were from controls in the Tokyo data set) genotyped by Illumina Human610-Quad BeadChip (Illumina, San Diego, CA). The LD map shown in Figure 1 was constructed based on the fine mapping data of the 52 SNPs (Supplementary Table 10) from the Single Nucleotide Polymorphism database (<http://www.ncbi.nlm.nih.gov/projects/SNP/>) on the 1266 Japanese controls (the same as controls in the Tokyo data set). The pattern of LD was

analyzed using 2 parameters, r^2 and $|D'|$,¹⁴ and the confidence interval of the $|D'|$ was also utilized.¹⁵

Statistical Analyses

Statistical significance of the association was evaluated for each SNP by logistic regression. *P* values under an additive model adjusted for 3 age categories (≤ 39 , 40–59, and ≥ 60 years), gender, and the risk alleles at rs2294008 in PSCA (Supplementary Figures 9–11). The significance level was set to .05 by Bonferroni correction for multiple testing, meaning $P = 8.9 \times 10^{-4}$ before correction for the Tokyo data set. Meta-analyses of the Tokyo data set and the Aichi and Korea replication data sets were performed using a random effects model.¹⁶ Haplotype-based association was tested by Fisher exact test. Haplotype phases in each individual were inferred by fastPHASE software.¹⁷ Other statistical analyses were carried out using the R suite (<http://www.r-project.org/>) and the StatXact 8 (Cytel Inc, Cambridge, MA). Population stratification of the Tokyo data set was examined previously by the STRUCTURE software,¹⁸ the Genomic Control, and mixture model methods,^{19,20} and no significant subpopulation was detected.⁷

In the association studies using 2-locus genotype data of rs4072037 and rs2294008, the biologic effect of the SNPs' risk allele was assumed to be recessive (rs4072037) or dominant (rs2294008), ie, the risk genotype for rs4072037 is AA and, for rs2294008, TT and TC (Figure 3). Risk factor variables consist of 4 categories based on the genotypes of rs4072037 and rs2294008. *P* value and OR and its 95% confidence interval (CI) for each category was obtained by logistic regression adjusted for age and gender.

Other Analyses

The materials and methods used in IGC association studies, genotyping, resequencing, and functional studies are described in Supplementary Materials and Methods and Supplementary Tables 9–11.

Results

Identification of the Susceptibility Region in Chromosome 1q22

Initially, we analyzed LD ($|D'|$) around the 2 marker SNPs based on the genotyping data on 680 control subjects. The criteria based on a confidence interval of $|D'|$ ¹⁵ was applied to find an LD block containing 12 SNPs (including rs2075570 and rs2070803) and 11 genes (Figure 2). The second analysis of high-density genotyping around this block was performed on 610 cases of DGC and 1266 controls (Tokyo data set) for 52 SNPs selected from the Single Nucleotide Polymorphism database. A solid 49kb-LD block was identified spanning 13 SNPs including rs2075570 and rs2070803. Eight SNPs in the block showed strong associations ($P < 1.0 \times 10^{-5}$)

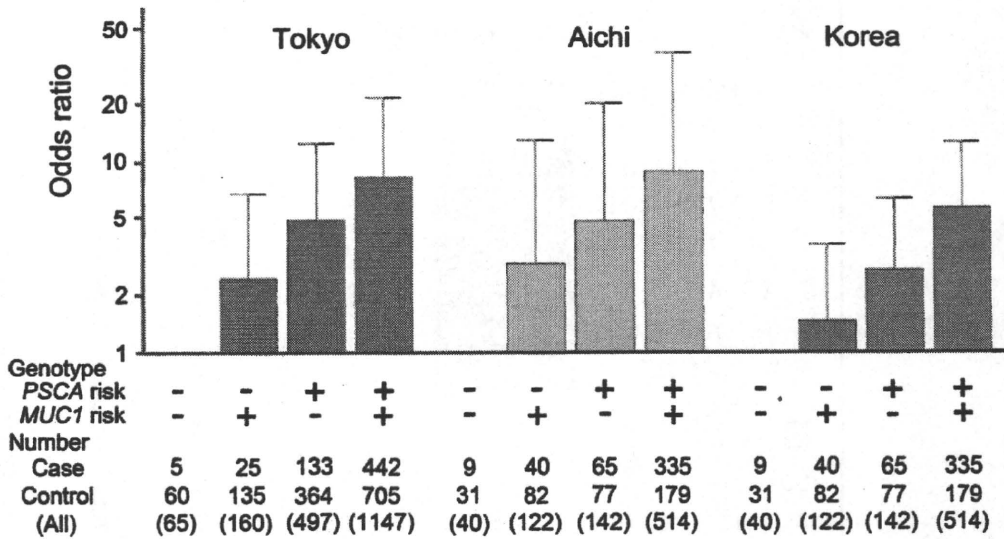


Figure 3. Association studies for DGC using 2-locus genotype data of rs4072037 in *MUC1* and rs2294008 in *PSCA*. The association studies were performed with a distinct model for each risk allele's effect, recessive for rs4072037 and dominant for rs2294008. Bar, upper bound of 95% confidence interval.

with DGC (Figure 1 and Table 1). Of the 8 SNPs, 4 were selected and genotyped on independent case-control sets in Japan (Aichi data set: 304 cases, 1467 controls) and in Korea (Korea data set: 455 cases, 372 controls), and the association was replicated in both data sets (Figure 1 and Table 1). A meta-analysis of the 3 case-control studies also showed significant correlation of the region: $P = 2.26 \times 10^{-12}$; OR, 1.71 for rs2075570 and $P = 4.33 \times 10^{-13}$; OR, 1.71 for rs2070803. Because this 1q22 region was originally identified by the GWAS on DGC,⁷ an association with IGC was examined on the 3 populations: 601, 274, and 415 cases from Tokyo, Aichi, and Korea, respectively, using the same control subjects analyzed for DGC. The 1q22 region was not significantly associated with IGC (Figure 1, Supplementary Figure 2). Full data of the association studies are shown in Supplementary Tables 1-4.

Polymorphisms in MUC1 Gene and Haplotype-Based Association Study

The 49-kilobase (kb) block contained 5 genes encoding keratinocyte associated protein 2 (*KRTCAP2*), tripartite motif protein 46 (*TRIM46*), mucin 1 (*MUC1*), thrombospondin 3 (*THBS3*), and metaxin 1 (*MTX1*). Based on their expression patterns and gene annotations, we prioritized *MUC1* for further analyses because *MUC1* is expressed in pit cells in the pit region, mucous neck cells in the neck region, chief (zymogenic) cells in the base region, and parietal cells in the neck and base regions of the gastric epithelium (Figure 4A, Supplementary Figure 1).²¹ Moreover, previous studies based on a candidate-gene approach reported an association between its polymorphisms and GC.⁸⁻¹¹

The resequencing of the *MUC1* gene identified a total of 7 polymorphisms in 48 Japanese individuals: 4 SNPs without rs numbers (numbers 1, 2, 4, and 7), 1 indel (No. 6, rs66597679), rs12411216 (No. 3), and rs4072037 (No. 5) (Figure 4B and Supplementary Table 5). The 7 were geno-

typed on 380 Japanese cases and 309 controls (Table 2), and, in a subsequent haplotype analysis, SNPs numbers 1 and 7 were removed from analysis because they were monomorphic in the 689 Japanese individuals. The remaining 5 SNPs were used for a haplotype-based association study, which revealed 3 major haplotypes, numbers 1-3, with ORs of 1.32, 0.90, and 0.65, respectively, and 1 minor haplotype, No. 4, with minor allele frequency of 0.0105 in cases and 0.0032 in controls (Table 3).

Functional Analyses of MUC1 SNPs

Seven transcriptional variants are registered as *MUC1* messenger RNA in the National Center for Biotechnology Information database (<http://www.ncbi.nlm.nih.gov/>) (Supplementary Figure 3), and the rs4072037 SNP ($P = 1.43 \times 10^{-11}$ and OR of 1.66 by meta-analysis of the 2 Japanese and 1 Korea data sets, Table 1) located in exon 2 of *MUC1* had been found to be related to the splicing site selection in the exon.¹² To identify the variants expressed in the stomach, we conducted RNA ligase-mediated rapid amplification of the 5' complementary DNA end procedure.

Our results showed that the major transcripts in the stomach are variants 2 and 3 (Figure 4B and Supplementary Figure 4) and that all the examined clones of variant 2 possessed G allele at rs4072037, in contrast to those of the variant 3 possessing the A allele, as reported previously (Supplementary Figure 5).¹² This suggests that rs4072037 is significantly involved in the splicing regulation of the second exon. In other words, it is likely that the SNP directly determines the relative dominance of the 2 major *MUC1* splicing variants, the variants 2 and 3, in the gastric epithelium.

As reported previously on the Caucasian population,¹² no polymorphisms other than rs4072037 were found in the region spanning from exon 1 to 2, which might affect the splicing of the second exon, by our resequencing of the

BASIC-ALIMENTARY TRACT

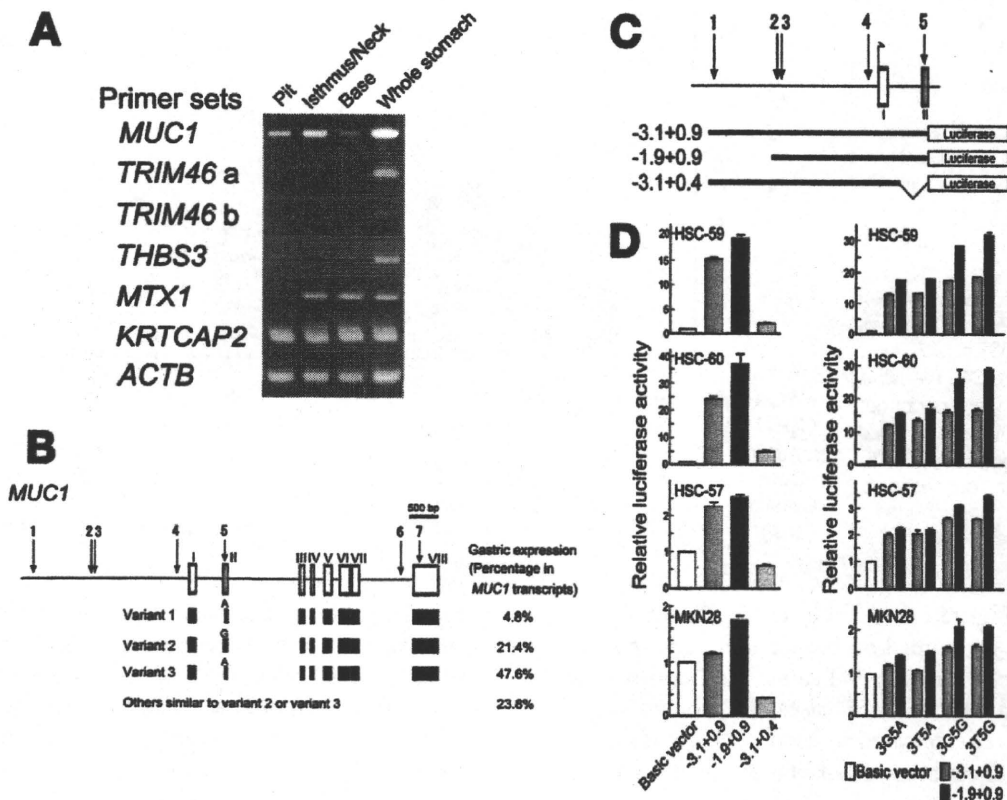


Figure 4. Functional analyses of *MUC1* and its SNPs. (A) Expression analysis on the 5 genes in the LD block associated with DGC using microdissected gastric samples (reverse-transcription polymerase chain reaction). (B) Seven polymorphisms in the *MUC1* gene identified by resequencing of 48 Japanese controls and *MUC1* transcriptional variants detected in RNAs from the gastric mucosa by RNA ligase-mediated rapid amplification of the 5' complementary DNA (cDNA) end procedure (5'RACE). SNP positions are indicated by arrows with numbers corresponding to Table 2 and Supplementary Table 5. The 5'RACE was conducted on a pooled gastric RNA sample from 21 Caucasian individuals. All the variant 2 clones contained exclusively the G allele of SNP No. 5 and all the variants 1 and 3 the A allele, without exception. Complete result of the 5'RACE is presented in Supplementary Figure 4. (C) *MUC1* genomic fragments examined in reporter assays. (D) Effect of SNP No.5 (rs4072037) on the transcriptional activity of the *MUC1* promoter (reporter assay). The transcriptional activity of the -3.1 to $+0.9$ region was significantly reduced by truncating the $+0.4$ to $+0.9$ region ($-3.1+0.4$) in gastric cancer cell lines HSC-59, HSC-60, HSC-57, and MKN28. The genomic fragments with G allele in the SNP (3G5G and 3T5G) showed higher reporter activity than that with A allele (3G5A and 3T5A).

MUC1 gene on 48 Japanese individuals (Figure 4B and Supplementary Table 5). As regards the splicing variation, the risk allele A at rs4072037, which is found in variants 1 and 3 (Supplementary Figure 5), causes a 9-amino acid deletion in the second exon and consequently modifies both the signal peptide and N-terminal amino acid of the mature

protein by changing the signal-peptide cleavage site.¹² This may change the intracellular trafficking and glycosylation and folding of the protein, leading to alteration in the function of the mature protein.

To examine the difference in the *MUC1* function among the variants, we evaluated in vitro functions of the

Table 2. Seven SNPs and Their Association With DGC Based on the Genotype Data of 380 Japanese Cases and 309 Controls

SNP no.	rs number	Major allele	Minor allele	Risk allele	MAF (case)	MAF (control)	OR ^a	95% CI	P value ^b
1		T	C		0.0000	0.0000			
2		C	T	C	0.1882	0.2039	1.11	0.85–1.44	.4945
3	12411216	G	T	G	0.1289	0.1851	1.53	1.14–2.06	.004344
4		G	A	A	0.0105	0.0032	3.28	0.69–15.49	.1998
5	4072037	A	G	A	0.1289	0.1857	1.54	1.15–2.07	.004275
6	66597679	AC	—	AC	0.1308	0.1869	1.53	1.14–2.05	.005225
7		C	T		0.0000	0.0000			

CI, confidence interval; MAF, minor allele frequency.

^aOdds ratio for risk allele.

^bP values obtained by Fisher exact test.

Table 3. Four Major Haplotypes Inferred and Their Association With DGC Based on the Genotype Data of 380 Japanese Cases and 309 Controls

Haplotype no.	SNP no.					Case ^a	Control ^b	OR	95% CI	P values	
	2	3	4	5	6					Fisher ^c	Permutation ^d
1	C	G	G	A	AC	0.6733	0.6084	1.32	1.06–1.65	.01501	.0483
2	T	G	G	A	AC	0.1884	0.2039	0.90	0.69–1.18	.4945	.9027
3	C	T	G	G	—	0.1278	0.1845	0.65	0.48–0.87	.004200	.0127
4	C	G	A	A	AC	0.0105	0.0032	3.28	0.69–15.49	.1998	.4058

CI, confidence interval.

^aFrequency of case.

^bFrequency of control.

^cP values obtained by Fisher exact test.

^dP values obtained by permutation test (100,000 permutations performed).

2 major variants expressed in the gastric epithelium: variants 2 and 3. Because the full-length product of *MUC1* is well-known for its cell growth-promoting activity in cancer cells,^{22,23} we individually transfected a cytomegalovirus promoter-driven complementary DNA of *MUC1* variant 2 or 3 to the MKN28 cells, which express *MUC1* at an undetectable level (data not shown). Examination of their cell growth by both cell counting and colorimetric methods suggested that variant 2 is more potent in growth-promoting activity than variant 3 (Supplementary Figures 6 and 7). Although the observed difference seems to be small, this level of normal range of individual variation is generally expected for a common genetic variant influencing a common disease susceptibility and is probably because of the difference in the signal peptide or the N-terminal structure of the mature protein encoded by each variant because the other portion of the amino acid sequence is common between the 2 variants.

Next, we investigated the function of the *MUC1* SNPs in the context of the haplotypes. We selected haplotype No. 1 as the major risk haplotype and haplotype No. 3 as the most protective haplotype and analyzed the functions of SNPs numbers 3 and 5, excluding SNP No. 6 from our functional analyses because its location in the intron 7 made it unlikely to be involved in the transcriptional regulation and/or alternative splicing of the gene. SNP numbers 2 and 4 were also excluded because they were found on both the risk and the protective haplotypes. Because the remaining 2 SNPs, numbers 3 and 5, do not change amino acid, we first examined, by a reporter assay, their effect on the transcriptional regulation of *MUC1*; the region spanning -1.9 to 0.9 kb relative to the *MUC1* transcription start site had a transcriptional activity (Figure 4C and D). The reporter assay on base-substituted constructs showed that, in all the gastric carcinoma cell lines examined, the fragments containing the G allele at rs4072037 (SNP No. 5), which is present only in the protective haplotype, has a higher transcriptional activity than that with an A allele present in the risk haplotype

(Figure 4D, right panel). The assay on truncated constructs showed that a removal of a $+0.4$ to $+0.9$ -kb region, which contains rs4072037, significantly diminishes the transcriptional activity (Figure 4D, left panel). We also confirmed in the reporter assay that the T allele of SNP No. 2, which is unique to haplotype No. 2 showing OR of 0.9 but no significant P value, has no effect (Supplementary Figure 8).

In sum, the results in this study and from previous reports by other investigators suggest that rs4072037 SNP has at least 2 functions: (1) regulation of the alternative splicing at the second exon and (2) modification of the transcriptional activity of the promoter. The association study in the context of LD and the functional study strongly implicate rs4072037 as a functional cause of the association between the 1q22 region and DGC susceptibility.

Association Studies for DGC Using 2-Locus Genotype Data of rs4072037 in *MUC1* and rs2294008 in *PSCA*

Finally, we examined the effect of 2 DGC susceptibility SNPs identified by our GWAS, rs4072037 in *MUC1* and rs2294008 in *PSCA*, both of which are functional, using Tokyo, Aichi, and Korea data sets. When a genetic model is tentatively selected for each locus by simply comparing P value, a recessive and dominant model was applied for rs4072037 and for rs2294008, respectively; the individuals possessing the risk genotype of both SNPs showed significant risk for developing DGC (eg, OR, 8.38 in Tokyo data set, Figure 3). Notably, individuals with protective alleles of both SNPs were observed only in controls (Supplementary Table 6).

Discussion

At chromosome 1q22, we focused on the region with strong LD around rs2075570 and rs2070803 using Gabriel et al's criteria.¹⁵ The region contains 5 genes: *TRIM46*, *THBS3*, *MTX1*, *KRTCAP2*, and *MUC1* (Figure 1). We prioritized the genes for the subject of

further studies by the first criterion (whether the gene is expressed in the gastric epithelial cells) and then by the second one (whether annotated function suggests its involvement in carcinogenesis). We observed transcripts of 4 of the 5 genes in microdissected samples of the gastric epithelium by reverse-transcription polymerase chain reaction, but no transcript of *TRIM46* was detectable there (Figure 4A). *THBS3* encoding a multifunctional extracellular matrix glycoprotein is expressed in multiple human tissues including the stomach,²⁴ and no evidence of a causal relation to carcinogenesis has been obtained. *MTX1* encodes a component of a preprotein import complex in the outer membrane of the mammalian mitochondrion.²⁵ If it is involved in carcinogenesis, the effect of its SNP would be reflected in many types of cancer, yet no such involvement has surfaced. *KRTCAP2* encodes a protein possessing transmembrane domain, showing multitissue expression.²⁶ Its function is unknown, and its relation to carcinogenesis has not been demonstrated.

In this study, we considered *MUC1* as a strong candidate for the gene responsible for the association of 1q22 with DGC because, in addition to several previous candidate gene analyses showing an association with *MUC1* polymorphisms and GC,⁸⁻¹¹ *MUC1* has been considered to possess an oncogenic property as described below.

Mucin family members are classified into 2 types, secreted or membranous, based on their localization, and *MUC1* is a transmembrane mucin.²⁷ *MUC1* is a multifunctional protein involved in mucosal lubrication, protection from pathogens, signal transduction, and cell-cell interaction.²⁷ *MUC1* was over-expressed in breast, ovarian, lung, pancreatic, and prostate cancers and was a marker of poor prognosis in gastric cancer.^{21,28} Several *in vivo* studies have provided evidence supporting its function in carcinogenesis. *MUC1* has a role in cell growth, anchorage independence, cell migration, antiapoptotic property, and drug resistance of cancer cells,^{22,29-33} all of which are accomplished through interaction with several signaling pathways,³⁴ although these lines of biologic evidence were obtained on the standard molecule containing tandem repeats (TR). Because the *MUC1* expressed in the gastric epithelium has no TR, it is possible that its function in gastric epithelial cells is different from that of the TR-containing product in other epithelial cells.³⁵⁻³⁷

Recently, however, it is supposed that *MUC1* has a protective function against environmental insults and acts against tumorigenesis in normal epithelial cells, which keep maintaining their cell polarity. In contrast, once the cells lose cell polarity in consequence of prolonged inflammation, *MUC1* promotes cell growth and acts for tumorigenesis.³⁸ It was also reported that *MUC1* functions as a growth factor receptor in human embryonic stem cells.³⁹ It is presumable that *MUC1* is involved in growth regulation of gastric stem cells and progeni-

tors, which are considered to be the origin of DGC. Like the function of *PSCA*, which is up-regulated in prostate and urinary bladder cancers but suppressed in gastric cancer,⁷ the *MUC1* function may differ between cell types, normal or malignant, and among different tissues. In the same manner as *PSCA*, *MUC1* is down-regulated in intestinal metaplasia of the gastric epithelium from which IGC arises.⁴⁰ If *MUC1* has some protective function in carcinogenesis, this down-regulation makes the stem and progenitor cells more susceptible to carcinogenic events. In any case, further research is needed to explore the pleiotropic functions of *MUC1*.

In this study, we demonstrated that rs4072037 has a role in transcriptional regulation and also in splicing site selection leading to the dominant variant determination of *MUC1* transcripts in gastric epithelial cells. If variant 3 is less functional in protection against DGC than variant 2, the possession of the A allele in the genome confers both quantitatively and qualitatively unfavorable consequences to *MUC1* function, which may result in additive risk for DGC susceptibility.

In our GWAS on DGC susceptibility, the 2 loci showing the highest statistical significance directed us to the 2 functional SNPs: rs4072037 in *MUC1* and rs2294008 in *PSCA*.⁷ It is noteworthy that both SNPs in the 2 genes appear to have dual functions: transcriptional regulation and signal-peptide modification.⁷ Further investigation is required to validate the role of *MUC1* in DGC susceptibility and details of the mechanism that links the risk haplotype tagged by rs4072037 to DGC development.

The risk allele A of rs4072037 is in strong LD with the small allele of the variable numbers of tandem repeats in the second intron of the *MUC1* both in Europeans and Japanese; more than 90% of chromosomes have a nonrecombinant haplotype in both populations (Ng et al¹² and Supplementary Table 7), and the small allele was associated with GC in the European population.^{8,9,12} However, the variable numbers of tandem repeats is unlikely to be the causal polymorphism for DGC susceptibility because the TRs are translated neither in normal nor malignant gastric epithelial cells (Supplementary Figure 4 and Supplementary Table 8).

This study has not only replicated the association of the *MUC1* SNP with GC in the Japanese and Korean populations, in addition to the previous reports on the Chinese and Caucasian population GCs,⁸⁻¹¹ but it has also disclosed that the association appears specific to DGC. Following discovery of the DGC-specific association of the *PSCA* polymorphism, this study has offered another piece of evidence to support distinct mechanisms for DGC and IGC development.

Although there was no significant interaction between the *MUC1* and *PSCA* SNPs for the DGC risk in our study (Figure 3, Supplementary Table 6, and data not shown), it is estimated that individuals with the double risk

genotype are the majority in Japanese (56%) and Korean (49%) populations with a significant OR, 8.38, in Japanese, as compared with the lowest risk category. GWAS and other emerging genome analysis tools may unveil a number of polymorphisms showing a significant statistical association, but it is important to identify functional SNPs potentially related to carcinogenesis. The accumulation of information on the functional SNPs, environmental factors, and their interactions, all of which are truly related to DGC susceptibility, will make the genotyping a more practical tool for evaluating the individual risk for DGC and offer effective prevention strategies in the future.

Supplementary Material

Note: To access the supplementary material accompanying this article, visit the online version of *Gastroenterology* at www.gastrojournal.org, and at doi: 10.1053/j.gastro.2010.10.058.

References

- Brenner H, Rothenbacher D, Arndt V. Epidemiology of stomach cancer. In: Verma M, ed. *Methods of molecular biology: cancer epidemiology*. Volume 472. New Jersey: Humana, 2009:467–477.
- Lauren P. The two histological main types of gastric carcinoma: diffuse and so-called intestinal-type carcinoma. An attempt at a histo-clinical classification. *Acta Pathol Microbiol Scand* 1965; 64:31–49.
- Chiba T, Marusawa H, Seno H, et al. Mechanism for gastric cancer development by *Helicobacter pylori* infection. *J Gastroenterol Hepatol* 2008;23:1175–1181.
- Schier S, Wright NA. Stem cell relationships and the origin of gastrointestinal cancer. *Oncology* 2005;69(Suppl 1):9–13.
- Henson DE, Dittus C, Younes M, et al. Differential trend in the intestinal and diffuse types of gastric carcinoma in the United States, 1973–2000—increase in the signet ring cell type. *Arch Pathol Lab Med* 2004;128:765–770.
- Rosai J. *Rosai and Ackerman's surgical pathology*. Edinburgh: Mosby, 2004.
- Study Group of Millennium Genome Project for Cancer. Genetic variation in *PSCA* is associated with susceptibility to diffuse-type gastric cancer. *Nat Genet* 2008;40:730–740.
- Carvalho F, Seruca R, David L, et al. *MUC1* gene polymorphism and gastric cancer—an epidemiological study. *Glycoconj J* 1997; 14:107–111.
- Silva F, Carvalho F, Peixoto A, et al. *MUC1* gene polymorphism in the gastric carcinogenesis pathway. *Eur J Hum Genet* 2001;9: 548–552.
- Xu Q, Yuan Y, Sun LP, et al. Risk of gastric cancer is associated with the *MUC1* 568 A/G polymorphism. *Int J Oncol* 2009;35: 1313–1320.
- Jia Y, Persson C, Hou L, et al. A comprehensive analysis of common genetic variation in *MUC1*, *MUC5AC*, *MUC6* genes and risk of stomach cancer. *Cancer Causes Control* 2010;21:313–321.
- Ng W, Loh AX, Teixeira AS, et al. Genetic regulation of *MUC1* alternative splicing in human tissues. *Br J Cancer* 2008;99:978–985.
- Japanese Gastric Cancer Association. Japanese classification of gastric carcinoma. 2nd English edition. *Gastric Cancer* 1998;1: 10–24.
- Nei M. *Molecular evolutionary genetics*. New York: Columbia University Press, 1987.
- Gabriel SB, Schaffner SF, Nguyen H, et al. The structure of haplotype blocks in human genome. *Science* 2002;296:2225–2229.
- DerSimonian R, Laird N. Meta-analysis in clinical trials. *Control Clin Trials* 1986;7:177–188.
- Scheet P, Stephens M. A fast and flexible statistical model for large-scale population genotype data: applications to inferring missing genotypes and haplotypic phase. *Am J Hum Genet* 2006; 78:629–644.
- Falush D, Stephens M, Pritchard JK. Inference of population structure using multilocus genotype data: linked loci and correlated allele frequencies. *Genetics* 2003;164:1567–1587.
- Bacanu SA, Devlin B, Roeder K. The power of genomic control. *Am J Hum Genet* 2000;66:1933–1944.
- Zhu X, Zhang S, Zhao H, et al. Association mapping, using a mixture model for complex traits. *Genet Epidemiol* 2002;23: 181–196.
- Senapati S, Sharma P, Bafna S, et al. The *MUC* gene family: their role in the diagnosis and prognosis of gastric cancer. *Histol Histopathol* 2008;23:1541–1552.
- Li Y, Liu D, Chen D, et al. Human DF3/*MUC1* carcinoma-associated protein functions as an oncogene. *Oncogene* 2003;4: 6107–6110.
- Tsutsumida H, Swanson BJ, Singh PK, et al. RNA interference suppression of *MUC1* reduces the growth rate and metastatic phenotype of human pancreatic cancer cells. *Clin Cancer Res* 2006;15:2976–2987.
- Adolph KW. Relative abundance of Thrombospondin 2 and Thrombospondin 3 mRNAs in human tissues. *Biochem Biophys Res Commun* 1999;258:792–796.
- Armstrong LC, Saenz AJ, Bornstein P. Metaxin 1 interacts with metaxin 2, a novel related protein associated with the mammalian mitochondrial outer membrane. *J Cell Biochem* 1999;74: 11–22.
- Bonkobara M, Das A, Takao J, et al. Identification of novel genes for secreted and membrane-anchored proteins in human keratinocytes. *Br J Dermatol* 2003;148:654–664.
- Gendler SJ. *MUC1*, the renaissance molecule. *J Mammary Gland Biol Neoplasia* 2001;6:339–353.
- Taylor-Papadimitriou J, Burchell J, Miles DW, et al. *MUC1* and cancer. *Biochim Biophys Acta* 1999;1455:301–313.
- Suwa T, Hinoda Y, Makiguchi Y, et al. Increased invasiveness of *MUC1* cDNA-transfected human gastric cancer MKN74 cells. *Int J Cancer* 1998;76:377–382.
- Raina D, Kharbanda S, Kufe D. The *MUC1* oncoprotein activates the anti-apoptotic phosphoinositide 3-kinase/Akt and Bcl-xL pathways in rat 3Y1 fibroblasts. *J Biol Chem* 2004;279:20607–20612.
- Ren J, Agata N, Chen D, et al. Human *MUC1* carcinoma-associated protein confers resistance to genotoxic anticancer agents. *Cancer Cell* 2004;5:163–175.
- Huang L, Chen D, Liu D, et al. *MUC1* oncoprotein blocks glycogen synthase kinase 3 β -mediated phosphorylation and degradation of β -catenin. *Cancer Res* 2005;65:10413–10422.
- Wei X, Xu H, Kufe D. Human mucin 1 oncoprotein represses transcription of the *p53* tumor suppressor gene. *Cancer Res* 2007;67:1853–1858.
- Singh PK, Hollingsworth MA. Cell surface-associated mucins in signal transduction. *Trends Cell Biol* 2006;16:467–476.
- Gendler SJ, Lancaster CA, Taylor-Papadimitriou J, et al. Molecular cloning and expression of human tumor-associated polymorphic epithelial mucin. *J Biol Chem* 1990;265:15286–15293.

36. Zrihan-Licht S, Vos HL, Baruch A, et al. Characterization and molecular cloning of a novel MUC1 protein, devoid of tandem repeats, expressed in human breast cancer tissue. *Eur J Biochem* 1994;224:787-795.
37. Baruch A, Hartmann M, Zrihan-Licht S, et al. Preferential expression of novel MUC1 tumor antigen isoforms in human epithelial tumors and their tumor-potentiating function. *Int J Cancer* 1997; 71:741-749.
38. Kufe DW. Mucins in cancer: function, prognosis and therapy. *Nat Rev Cancer* 2009;9:874-885.
39. Hikita ST, Kosik KS, Clegg DO, et al. MUC1* mediates the growth of human pluripotent stem cells. *PLoS One* 2008;3:e3312.
40. Silva E, Teixeira A, David L, et al. Mucins as key molecules for the classification of intestinal metaplasia of the stomach. *Virchows Arch* 2002;440:311-317.

Received May 8, 2010. Accepted October 26, 2010.

Reprint requests

Address requests for reprints to: Teruhiko Yoshida, MD, Genetics Division, National Cancer Center Research Institute, 5-1-1 Tsukiji,

Chuo-ku, Tokyo 104-0045, Japan. e-mail: tyoshida@ncc.go.jp; fax: (81) 3-3541-2685.

Acknowledgments

The authors thank Sachiyo Mimaki, Mineko Ushiyama, Chie Naito, Yoko Odaka, Misuzu Okuyama, Miki Watanabe, and Hidemi Ito for their technical contributions and Seiji Ito for the clinical data collection of the Aichi data set.

Conflicts of Interest

The authors disclose no conflicts.

Funding

Supported in Japan by the program for promotion of Fundamental Studies in Health Sciences of the National Institute of Biomedical Innovation (NiBio); in Aichi, supported by a Grant-in-Aid for Scientific Research from the Ministry of Education, Science, Sports, Culture and Technology of Japan and by a Grant-in-Aid for the Third Term Comprehensive 10-Year Strategy for Cancer Control from the Ministry of Health, Labour and Welfare of Japan; and, in Korea, part of the study was supported by grant 0710340 from the National Cancer Center, Korea.

Chemoprevention by nonsteroidal anti-inflammatory drugs eliminates oncogenic intestinal stem cells via SMAC-dependent apoptosis

Wei Qiu^a, Xinwei Wang^a, Brian Leibowitz^a, Hongtao Liu^a, Nick Barker^b, Hitoshi Okada^c, Naohide Oue^d, Wataru Yasui^d, Hans Clevers^b, Robert E. Schoen^a, Jian Yu^{a,1}, and Lin Zhang^{a,1}

^aUniversity of Pittsburgh Cancer Institute and Departments of Pharmacology and Chemical Biology, Pathology, and Medicine, University of Pittsburgh School of Medicine, Pittsburgh, PA 15213; ^bThe Hubrecht Institute for Developmental Biology and Stem Cell Research, 3584 CT, Utrecht, The Netherlands; ^cThe Campbell Family Institute for Breast Cancer Research, Ontario Cancer Institute, University Health Network, Toronto, ON, Canada M5G 2C1; and ^dDepartment of Molecular Pathology, Hiroshima University Graduate School of Biomedical Sciences, Hiroshima 734-8553, Japan

Edited* by Bert Vogelstein, The Sidney Kimmel Comprehensive Cancer Center at Johns Hopkins, Baltimore, MD, and approved October 6, 2010 (received for review July 18, 2010)

Nonsteroidal anti-inflammatory drugs (NSAIDs) such as sulindac effectively prevent colon cancer in humans and rodent models. However, their cellular targets and underlying mechanisms have remained elusive. We found that dietary sulindac induced apoptosis to remove the intestinal stem cells with nuclear or phosphorylated β -catenin in $APC^{Min/+}$ mice. NSAIDs also induced apoptosis in human colonic polyps and effectively removed cells with aberrant Wnt signaling. Furthermore, deficiency in SMAC, a mitochondrial apoptogenic protein, attenuated the tumor-suppressive effect of sulindac in $APC^{Min/+}$ mice by blocking apoptosis and removal of stem cells with nuclear or phosphorylated β -catenin. These results suggest that effective chemoprevention of colon cancer by NSAIDs lies in the elimination of stem cells that are inappropriately activated by oncogenic events through induction of apoptosis.

Prevention of human cancers by using chemical agents or dietary manipulation represents a promising anticancer strategy (1, 2). Widely used nonsteroidal anti-inflammatory drugs (NSAIDs) such as sulindac and aspirin effectively prevent colon cancer in humans and rodent models (3, 4). However, their cellular targets and underlying mechanisms have remained elusive. Colorectal tumorigenesis is initiated by genetic alterations in the *APC* tumor suppressor pathway through Wnt signaling, leading to accumulation of β -catenin and its subsequent nuclear translocation (5). This process has been largely recapitulated in animal models such as $APC^{Min/+}$ mice, which contain an *APC* mutation and exhibit intestinal adenoma formation (6). Emerging evidence suggests that initial neoplastic proliferation in $APC^{Min/+}$ mice impinges upon loss of *APC* in intestinal stem cells (7, 8), including crypt base columnar (CBC) cells near the crypt bottom, as well as those located in position 4–6 (+4) counting from the crypt bottom (9). Several intestinal stem cell markers have been identified, such as *Lgr5* (10), *Bmi1* (8), and *OLFM4* (11).

Substantial evidence indicates that the chemopreventive effects of NSAIDs are mediated by induction of apoptosis, a safeguard mechanism protecting against neoplastic transformation (12, 13). Our previous work established that NSAIDs induce mitochondria- and Bax-dependent apoptosis in colon cancer cells (14), and that SMAC (second mitochondria-derived activator of caspase), a mitochondrial apoptogenic protein (15), is an essential downstream mediator of Bax in NSAID-induced apoptosis (16, 17). In this study, we investigated the role of intestinal stem cell apoptosis in chemoprevention by NSAIDs. Our data suggest a critical role of SMAC-mediated apoptosis in removing early neoplastic stem cells in cancer chemoprevention by NSAIDs.

Results

Sulindac Treatment Induced Apoptosis in Intestinal Stem Cells of $APC^{Min/+}$ Mice. Dietary supplementation with NSAIDs such as sulindac for several months prevents adenoma formation in the

small intestine of $APC^{Min/+}$ mice (18). To study the role of apoptosis in chemoprevention by NSAIDs, we first determined the time window for analyzing sulindac-induced apoptosis in $APC^{Min/+}$ mice because of the rapid and transient nature of apoptotic events. We found that sulindac given for only 1 wk markedly induced apoptosis detected by TUNEL staining in the small intestinal crypts of $APC^{Min/+}$ mice, with 22.1% of crypts containing at least one TUNEL-positive cell, compared with only 4.0% in mice receiving control diet (Fig. 1A). Importantly, this short exposure reduced the number of macroadenomas by 66.7% (Fig. 1B), consistent with observations made by others (19). Sulindac treatment for 2 wk or longer further decreased polyp numbers (Fig. S1A). However, TUNEL staining detected little apoptosis at 2 wk or later after treatment (Fig. 1A and Fig. S1B), suggesting that most of the apoptosis had occurred earlier. As previously shown (20), sulindac treatment did not significantly affect polyp formation in the colon of $APC^{Min/+}$ mice. These observations indicate that sulindac rapidly induces apoptosis in the small intestine of $APC^{Min/+}$ mice, and this early apoptosis may be responsible for effective chemoprevention. Therefore, 1-wk sulindac treatment was chosen for most of the subsequent experiments.

In light of recent reports that *APC* loss in intestinal stem cells efficiently promotes adenoma formation (7, 8), we further determined the types of cells undergoing apoptosis in $APC^{Min/+}$ mice following 1 wk of sulindac treatment. Remarkably, a majority of TUNEL-positive cells were the wedge-shaped CBC cells (62.7%) and +4 cells (27.5%), whereas apoptotic cells were rare (<10%) at higher positions in the crypts (Fig. 1C and D and Fig. S2). Upon introducing the *Lgr5*-EGFP lineage marking allele (10) into $APC^{Min/+}$ mice, we found that sulindac treatment induced apoptosis in *Lgr5*-expressing cells of *Lgr5*-EGFP/ $APC^{Min/+}$ mice, but not WT mice (Fig. 1C and E and Fig. S3). The fraction of *Lgr5*-positive crypts containing one or more TUNEL-positive cells increased from 4.32% in the control mice to 17.60% in the sulindac-treated mice (Fig. 1E). We confirmed that the *Lgr5*-marked CBC cells and apoptotic cells at the crypt base were interspersed between MMP7-positive Paneth cells (Fig. 1C and Figs. S3B and S4) (21). Active caspase 3 staining verified the induction of apoptosis in these cells (Fig. 1F and Fig. S3C). Interestingly, apoptotic CBC cells were found to be clustered in

Author contributions: W.Q., J.Y., and L.Z. designed research; W.Q., X.W., B.L., and H.L. performed research; N.B., H.O., N.O., W.Y., H.C., and R.E.S. contributed new reagents/analytic tools; W.Q., J.Y., and L.Z. analyzed data; and W.Q., J.Y., and L.Z. wrote the paper.

The authors declare no conflict of interest.

*This Direct Submission article had a prearranged editor.

¹To whom correspondence may be addressed. E-mail: zhanglx@upmc.edu or yuj2@upmc.edu.

This article contains supporting information online at www.pnas.org/lookup/suppl/doi:10.1073/pnas.1010430107/-DCSupplemental.

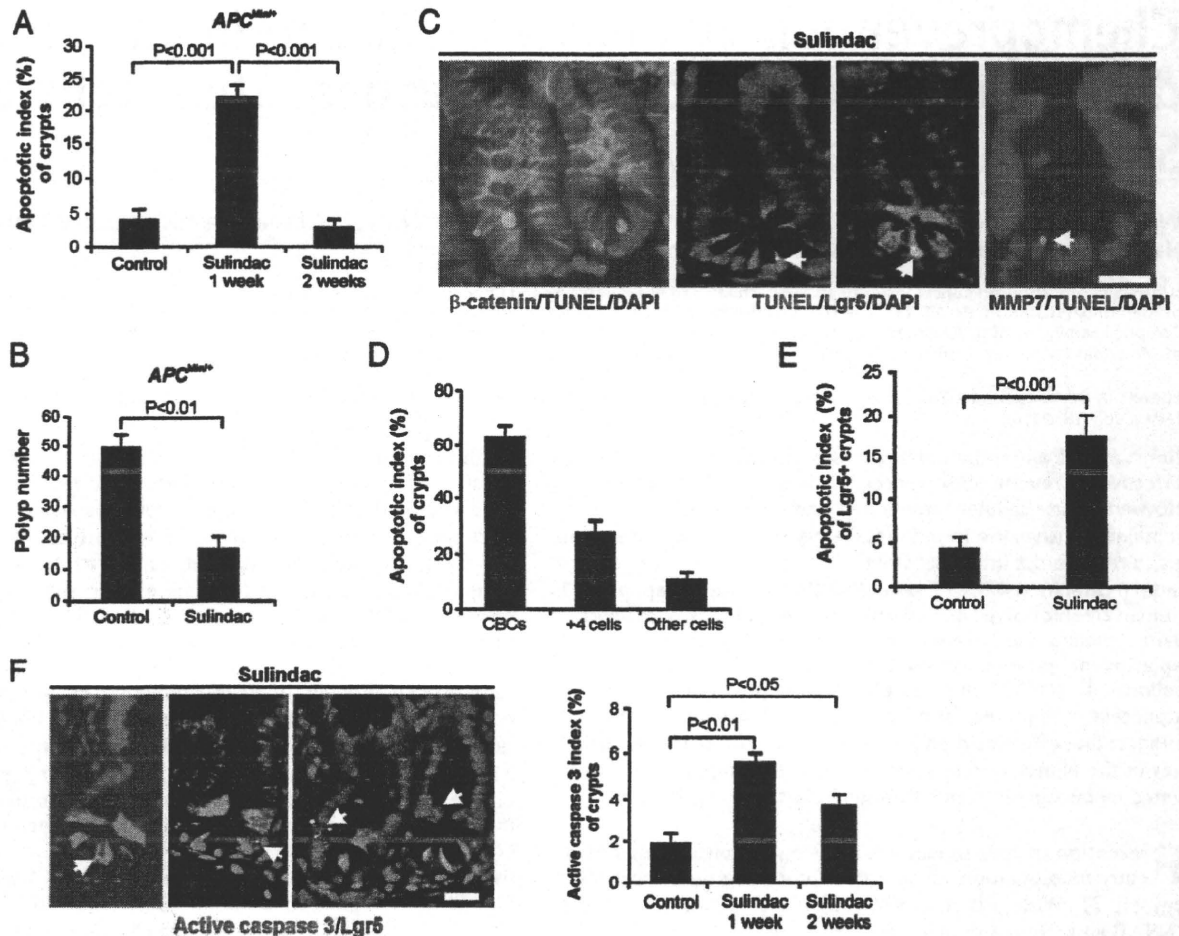


Fig. 1. Short-term sulindac administration induced apoptosis in the intestinal stem cells and suppressed adenoma formation in $APC^{Min/+}$ mice. Ten-week-old $APC^{Min/+}$ mice were fed with control or sulindac-containing (20 mg/kg/d) AIN93G diet for 1 or 2 wk and killed immediately after treatment. Intestinal polyp phenotypes, β -catenin localization, and apoptosis were analyzed. (A) Small intestinal sections from the treated mice were analyzed for apoptosis by TUNEL staining. The fractions of crypts containing at least one TUNEL-positive cell were determined. (B) Numbers of small intestinal polyps (≥ 0.5 mm in diameter) were counted following sulindac treatment for 1 wk. (C) Staining of indicated makers in $APC^{Min/+}$ mice treated with sulindac for 1 wk. For Lgr5 (EGFP) staining, $APC^{Min/+}$ mice containing the Lgr5-EGFP lineage marking allele ($Lgr5-EGFP/APC^{Min/+}$ mice) were analyzed. Lgr5 marks CBC cells and occasionally +4 cells, whereas MMP7 labels Paneth cells. DAPI (blue) was used for nuclear counter staining. Arrows indicate example TUNEL-positive CBCs (Lgr5-positive or MMP7-negative). (D) Quantification of TUNEL-positive cells based on locations in the crypts. Apoptotic index represents the fraction of crypts containing one or more TUNEL-positive cells. (E) Quantification of Lgr5-positive crypts containing one or more TUNEL-positive cells in $Lgr5-EGFP/APC^{Min/+}$ mice treated with control or sulindac diet for 1 wk. (F) Left: Staining of Lgr5 (red) and active caspase 3 (green) in $APC^{Min/+}$ mice treated with sulindac for 1 wk, with arrows indicating double positive cells. Right: Quantification of crypts containing one or more active caspase 3-positive cells. Values in A, B, and D–F are means \pm SD ($n = 6$ in each group). At least 500 crypts from each animal were analyzed. (Scale bars: 15 μ m.)

several neighboring Lgr5-positive crypts (Fig. 1 C and F and Fig. S3A), probably reflecting clonal expansion of the intestinal stem cells in which an early oncogenic event(s) occurred. These data demonstrate that intestinal stem cells are targeted for apoptosis induction following NSAID treatment.

Sulindac Treatment Removed Intestinal Stem Cells with β -Catenin Accumulation and Suppressed β -Catenin Phosphorylation. Intestinal polyp formation in $APC^{Min/+}$ mice is always accompanied by loss of the remaining WT APC allele (22), leading to deregulation of Wnt signaling and nuclear translocation of β -catenin (23). We therefore reasoned that sulindac may preferentially induce apoptosis in stem cells with nuclear β -catenin. Indeed, nuclear β -catenin was found in 1.92% of intestinal crypts in the control mice, including both the CBC and +4 cells, but rarely ($<0.01\%$ crypts) in other areas of the intestinal epithelium, or in the crypts of WT mice (Fig. 2A). Sulindac treatment for only 1 wk reduced the number of crypts containing cells with nuclear β -catenin by 75% (Fig. 2A). Interestingly, a vast

majority (98%, 0.47%/0.48%) of identifiable CBC and +4 cells with nuclear β -catenin in sulindac-treated $APC^{Min/+}$ mice were TUNEL-positive at this time point (Fig. 2A and B).

It has been shown that β -catenin nuclear translocation can be promoted by phosphorylation at Ser552 in the +4 cells (24). We found that the number of cells positive for β -catenin Ser552 phosphorylation (p- β -catenin), including mostly +4 and above +4 cells that did not express Lgr5 and some (11.4%) Lgr5-expressing cells (Fig. S5), was ninefold higher in $APC^{Min/+}$ mice compared with that in WT mice. Sulindac treatment significantly reduced cells with p- β -catenin (Fig. 2C), and induced rapid and significant apoptosis in these cells (Fig. 2D). These results suggest that sulindac treatment rapidly removes intestinal stem cells or progenitors with aberrant activation of Wnt signaling through induction of apoptosis.

NSAID Treatment Induced Apoptosis in Human Colonic Polyps and Removed Cells with Aberrant Wnt Signaling. To test the relevance of these observations in human patients, we analyzed colonic polyps

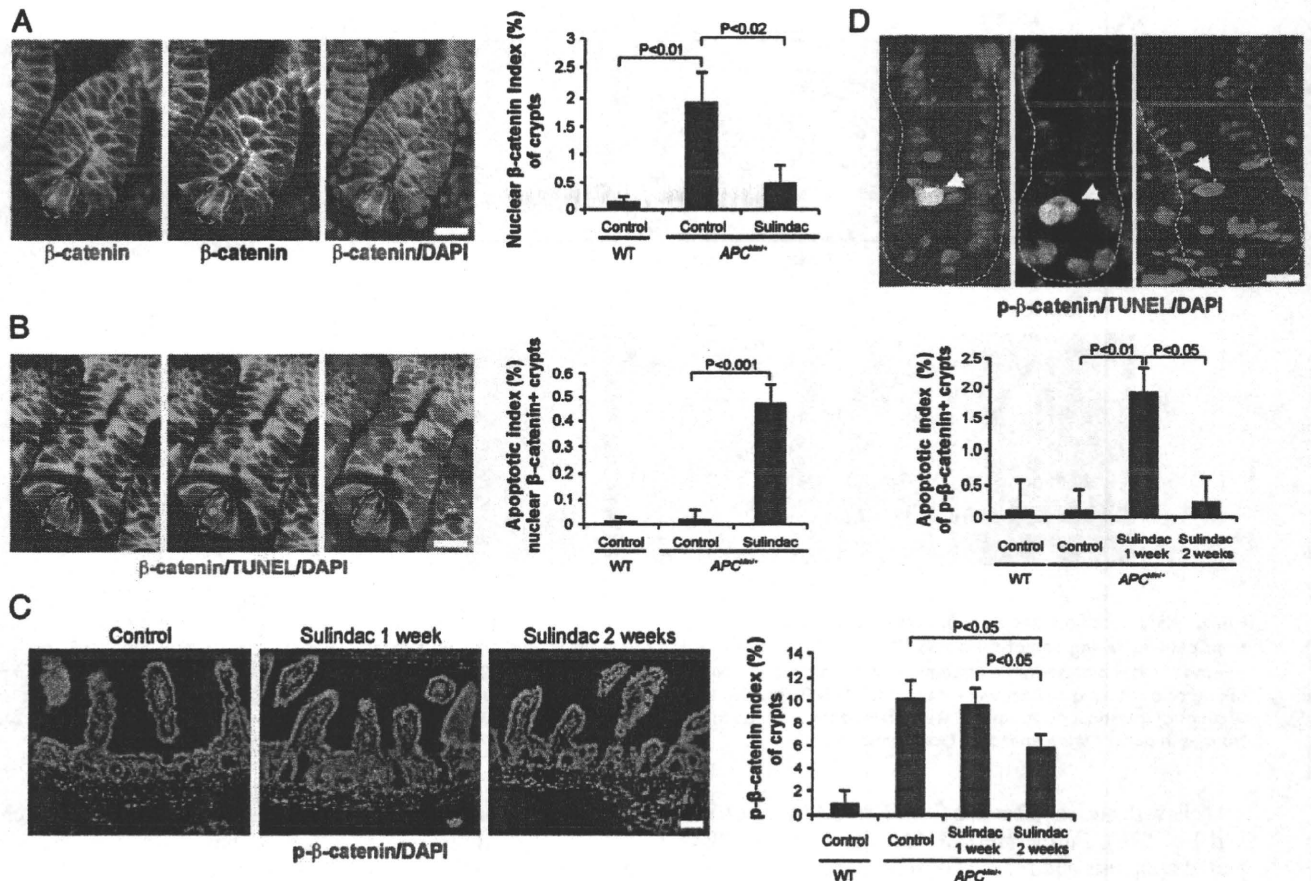


Fig. 2. Sulindac treatment removed the intestinal cells with nuclear or phospho-β-catenin via apoptosis. WT and *APC^{Min/+}* mice were fed with control or sulindac-containing (20 mg/kg/d) diet for 1 or 2 wk and killed immediately after treatment. Small intestinal sections from the mice were analyzed for β-catenin localization, β-catenin Ser552 phosphorylation (p-β-catenin), and apoptosis (TUNEL) by immunostaining. (A) Analysis of β-catenin localization. *Left:* Staining of β-catenin (green or white) and DAPI (blue) in *APC^{Min/+}* mice treated with sulindac for 1 wk. Circles mark representative CBCs with nuclear β-catenin. *Right:* Quantification of crypts with nuclear β-catenin in WT or *APC^{Min/+}* mice treated with control or sulindac diet for 1 wk. (B) Analysis of β-catenin localization and apoptosis. *Left:* Staining of β-catenin (green), TUNEL (red), and DAPI (blue) in *APC^{Min/+}* mice treated with sulindac for 1 wk. Circles mark example CBCs with nuclear β-catenin that were undergoing apoptosis. *Right:* Quantification of crypts positive for both nuclear β-catenin and TUNEL in WT and *APC^{Min/+}* mice treated with control or sulindac diet for 1 wk. (C) Analysis of β-catenin phosphorylation. *Left:* Staining of p-β-catenin (red) and DAPI (blue) in *APC^{Min/+}* mice treated with control or sulindac diet for 1 or 2 wk. *Right:* Quantification of crypts containing p-β-catenin-positive cells. (D) Analysis of β-catenin phosphorylation and apoptosis. *Upper:* Staining of p-β-catenin (red), TUNEL (green), and DAPI (blue) in *APC^{Min/+}* mice treated with sulindac for 1 wk. Arrows indicate TUNEL and p-β-catenin double-positive cells. *Lower:* Quantification of crypts containing apoptotic cells in WT or *APC^{Min/+}* mice treated with control or sulindac diet for 1 or 2 wk. Values in A–D are means ± SD ($n = 6$ in each group). At least 500 crypts from each animal were analyzed. (Scale bars: 15 μm)

in patients taking NSAIDs. The percentage of colonic crypts containing TUNEL-positive apoptotic cells increased by more than 10-fold (from 5.04% to 51.9%) in the patients taking NSAIDs compared with those not taking NSAIDs (Fig. 3A and B and Fig. S6). TUNEL-positive cells could be detected among those stained positive for OLFM4, a Wnt target and a CBC cell marker (11, 25) (Fig. 3C). Interestingly, we found that the number of p-β-catenin-positive cells decreased drastically (by more than sixfold) in patients taking NSAIDs (Fig. 3D). These data suggest that NSAIDs selectively induce apoptosis in human intestinal polyps with aberrant Wnt signaling.

SMAC Deficiency Attenuated the Chemopreventive Effect of Sulindac. Our previous work revealed that SMAC, a mitochondrial apoptogenic protein released into cytosol during apoptosis execution (15), is essential for NSAID-induced apoptosis in colon cancer cells (16, 17). To determine whether such a mechanism operates in vivo, age- and sex-matched cohorts of *APC^{Min/+}* mice with WT SMAC (*APC^{Min/+}*) or SMAC-KO (*SMAC^{-/-}/APC^{Min/+}*) were generated and subjected to sulindac treatment for 1 wk. SMAC

deficiency significantly attenuated the chemopreventive effect of sulindac in *APC^{Min/+}* mice (50.2% vs. 69.6%; $P < 0.01$; Fig. 4A and Fig. S7A). A slight increase in polyp number in SMAC-deficient *APC^{Min/+}* mice was observed, and taken into the consideration. Anatomic stratification revealed that the differences were mainly in the middle and distal regions, but not in the proximal region of small intestine (Fig. 4B). No significant difference in polyp size was found.

SMAC Deficiency Impaired Sulindac-Induced Apoptosis and Suppression of Nuclear β-Catenin Accumulation. Following 1 wk of sulindac treatment, the number of crypts with TUNEL-positive CBC/+4 cells was significantly lower in the *SMAC^{-/-}/APC^{Min/+}* mice than in *APC^{Min/+}* mice (9.9% vs. 22.1%; $P < 0.005$; Fig. 4C and Fig. S7B). Apoptosis in the crypts decreased significantly in both strains following 2 wk of sulindac treatment (Fig. 4C and Fig. S7C). Similarly, the number of cells or crypts with nuclear β-catenin was significantly higher in *SMAC^{-/-}/APC^{Min/+}* mice compared with that in *APC^{Min/+}* mice (1.33% vs. 0.48%; $P < 0.05$; Fig. 4D), which was correlated with a significant decrease of apoptosis in the CBC/

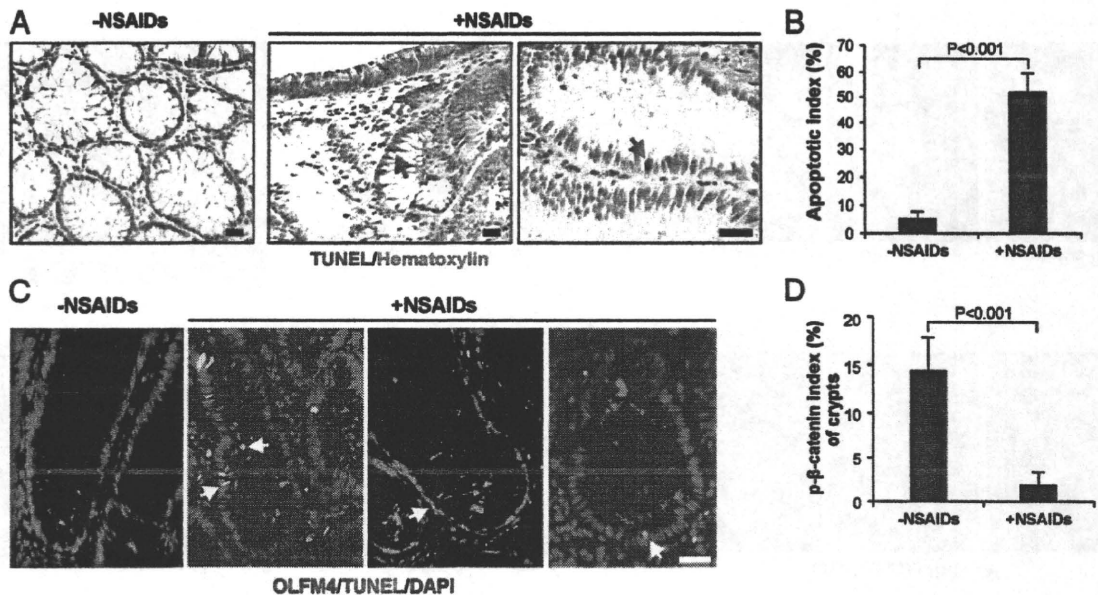


Fig. 3. NSAIDs induced apoptosis in human colonic polyps and removed cells with activated Wnt signaling. (A) TUNEL staining (brown) of intestinal polyps from patients taking or not taking NSAIDs. Arrows indicate TUNEL-positive apoptotic cells. (B) Quantification of crypts containing TUNEL-positive cells. Apoptotic index represents the percentage of intestinal crypts containing one or more TUNEL-positive cells. (C) Sections of intestinal polyps from four patients taking or not taking NSAIDs were stained for TUNEL (green), OLFM4 (red), and DAPI (blue). Arrows indicate TUNEL and OLFM4 double-positive cells. (D) Sections of intestinal polyps as in C were stained for p- β -catenin and quantified. Values in B and D are means \pm SD ($n = 4$ in each group). At least 200 crypts from each patient were analyzed. (Scale bars: 15 μ m).

+4 cells with nuclear β -catenin (0.22% vs. 0.47%; $P < 0.05$; Fig. 4E and Fig. S7B). Furthermore, SMAC deficiency significantly impaired apoptosis and removal of p- β -catenin-positive cells in the crypts (Fig. 4F and G). In addition, sulindac treatment did not affect SMAC expression in the mucosa of $APC^{Min/+}$ mice (Fig. S8A) and in colon cancer cells that undergo SMAC-dependent apoptosis (17) (Fig. S8B). These results demonstrate that SMAC-mediated apoptosis in the intestinal stem cells with aberrant activation of Wnt signaling directly contributes to chemoprevention.

Discussion

Neoplastic transformation appears to be driven by accumulation of genetic and epigenetic alterations in tissue stem cells or progenitors with pluripotency and regenerative potential (26, 27). Our results indicate that CBC and +4 intestinal stem cells accumulating nuclear or p- β -catenin are selectively removed by NSAIDs in $APC^{Min/+}$ mice through apoptosis induction, which translates into effective tumor prevention. Apoptosis in intestinal epithelial cells proceeds rapidly, typically within days (28), which may explain why we could detect sulindac-induced apoptosis only at an early time point. The partial effect of SMAC deficiency on sulindac-mediated chemoprevention is consistent with incomplete block of sulindac-induced apoptosis in SMAC-KO mice (Fig. 4C) and cells (17), and involvement of additional mechanisms including COX inhibition (29). The upstream events that activate Bax to trigger SMAC release following sulindac treatment remain to be delineated, and may involve death receptor signaling as suggested by several recent studies (30, 31).

Several characteristics of stem cells may explain the preferential killing of oncogenic stem cells by sulindac. Stem cells express high levels of "stemness" factors including the oncoprotein c-Myc (32), a well known apoptosis inducer (33). Therefore, stem cells with oncogenic alterations, such as loss of *APC*, may be more sensitive to NSAID-induced apoptosis, relative to differentiated cells with such alterations. It is also possible that stem cells with oncogenic alterations are simply more prevalent than differentiated cells with such alterations, because stem cells can

regenerate and permanently keep acquired genetic changes, whereas differentiated cells with these changes may quickly disappear because of their rapid turnover.

Long-term use of NSAIDs, in particular COX2-specific inhibitors, is associated with side effects, which has stimulated active pursuit of new targets and combination strategies for cancer chemoprevention (34). Induction of apoptosis in oncogenic stem cells is likely to be a useful marker for successful cancer prevention, and may hold the promise for identifying novel and improved cancer chemopreventive agents. Small-molecule SMAC mimetics, which are in clinical development and can sensitize colon cancer cells to NSAID-induced apoptosis (16), may be useful as sensitizers of NSAIDs for safer and more effective cancer chemoprevention.

Methods

Mice and Treatment. All animal experiments were approved by the Institutional Animal Care and Use Committee at University of Pittsburgh. The SMAC-KO mice on a mixed background (129/C57BL/6) (35) were backcrossed to C57BL/6 background for 10 generations. Female SMAC^{-/-} mice were crossed with $APC^{Min/+}$ mice (Jackson Laboratory) to generate SMAC^{-/-}/ $APC^{Min/+}$ male mice, which were crossed to SMAC^{-/-} mice to generate $APC^{Min/+}$ littermates with homozygous WT (^{+/+}) or null (i.e., KO; ^{-/-}) SMAC alleles. The previously described *Lgr5-EGFP* (*Lgr5-EGFP-IRES-creERT2*) mice (10) were crossed with $APC^{Min/+}$ mice to generate *Lgr5-EGFP*/ $APC^{Min/+}$ mice. All mice were housed in micro isolator cages in a room illuminated from 7:00 AM to 7:00 PM (i.e., 12-h/12-h light-dark cycle), and allowed access to water and chow ad libitum. Genotyping was performed as previously described for SMAC (35) and for *Lgr5* (10). *APC* genotyping was according to the Jackson Laboratory protocol.

Treatment and Tumor Analysis. Ten-week-old and sex-matched $APC^{Min/+}$ mice with different SMAC and *Lgr5* genotypes were fed with control or experimental AIN93G diet (Dyets) containing 200 ppm (approximately 20 mg/kg/d) of sulindac (Sigma) for 1, 2, or 22 wk. Mice were killed immediately after treatment. Dissection of small intestine and histological analysis of adenomas (polyps; >0.5 mm in diameter) were performed as previously described (36). The adenoma counts were performed under a dissection microscope at various times following sulindac treatment.

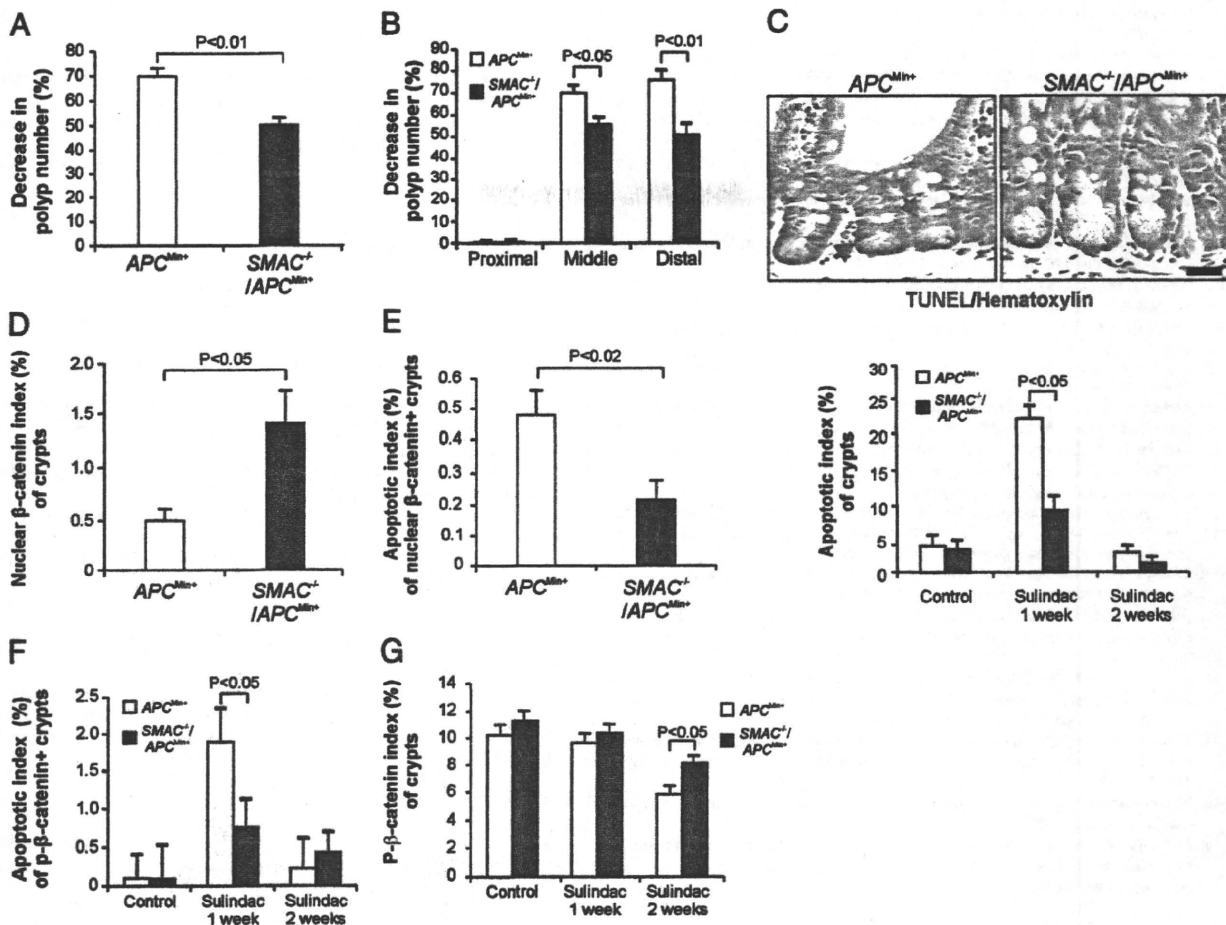


Fig. 4. SMAC deficiency attenuated the chemopreventive effect of sulindac in *APC^{Min/+}* mice by blocking apoptosis in the intestinal stem cells. Age- and sex-matched parental (*APC^{Min/+}*) and SMAC-deficient *APC^{Min/+}* mice (*SMAC^{-/-}/APC^{Min/+}*) were fed with control or sulindac-containing (20 mg/kg/d) diet for 1 or 2 wk and killed immediately after treatment. Intestinal polyp phenotypes, β -catenin localization, β -catenin Ser552 phosphorylation (p- β -catenin), and apoptosis were analyzed and compared. (A) Polyp (≥ 0.5 mm in diameter) number reduction in the treated mice. (B) Distribution of polyp number reduction in three different regions in the small intestine of the treated mice. (C) *Upper*: Staining of TUNEL (brown) and hematoxylin (blue) in the mice treated with sulindac for 1 wk. Arrows indicate example TUNEL-positive cells. (Scale bar: 15 μ m). *Lower*: Quantification of crypts containing one or more TUNEL-positive cells in the treated mice. (D) Fractions of crypts containing one or more CBC cells with nuclear β -catenin. (E) Fractions of crypts containing one or more TUNEL-positive cells with nuclear β -catenin. (F) Fractions of crypts containing one or more p- β -catenin and TUNEL double-positive cells. (G) Fractions of crypts containing one or more p- β -catenin-positive cells. Values are means \pm SD; $n = 6$ in each group in A–D; $n = 4$ in each group in E–G. At least 500 crypts from each animal were analyzed.

Immunostaining. Tissue sections (5 μ m) were deparaffinized, rehydrated, and treated with 3% hydrogen peroxide, followed by antigen retrieval in boiling 0.1 M citrate (pH 6.0) buffer for 10 min twice. The sections were then blocked by 20% goat/rabbit serum for 30 min. TUNEL staining was performed by using an ApopTag Kit (Chemicon International) according to the manufacturer's protocol. Immunostaining was performed as previously described for MMP7 (21), active caspase 3 (37), and OLFM4 (25). EGFP staining was performed at 4 °C overnight using a mouse anti-EGFP antibody (Santa Cruz Biotechnology), with Alexa 594 (Invitrogen) for signal detection. β -Catenin staining was done at 4 °C overnight using a mouse anti- β -catenin antibody (BD Biosciences), with Alexa 488 (Invitrogen) for signal detection. Staining of p- β -catenin Ser552 was performed as described (24). For double staining, TUNEL staining was performed following EGFP, β -catenin, p- β -catenin, OLFM4, or MMP-7 staining. EGFP staining was performed before MMP7, p- β -catenin, or active caspase 3 staining. Cells with positive staining were scored in at least 500 crypt sections and reported as mean \pm SD.

Clinical Samples. Frozen specimens of polyps from four patients taking NSAIDs and four patients not taking NSAIDs were obtained from the Digestive Disease Tissue Resource of the University of Pittsburgh. Acquisition of tissue samples was approved by the institutional review board at the University of Pittsburgh and written informed consent was received from each patient. Paraffin blocks and sections were prepared as previously described (21) and analyzed by immunostaining.

Two male and two female subjects were represented in each category, with ages ranging from 50 to 65 y in the NSAID group and 58 to 75 y in the non-NSAID group. Subjects taking NSAIDs reported use ranging from one to three tablets per week to greater than seven tablets per week during the preceding year. The specific NSAIDs in use were not recorded. All patients had advanced adenomas by virtue of having polyps at least 1 cm in size. Four patients had tubulovillous histology and four had tubular adenomas.

Statistical Analysis. Statistical analyses were carried out using GraphPad Prism IV software. P values were calculated by the Student's t test. $P < 0.05$ was considered to be significant. The means \pm 1 SD are displayed in the figures where applicable.

ACKNOWLEDGMENTS. We thank Dr. Monica E. Buchanan and other members of the L.Z. and J.Y. laboratories for helpful discussion and advice, Dr. Ronald A. DePinho at the Dana-Farber Cancer Institute (Boston, MA) for providing rederived *Lgr5-EGFP* mice, and Dr. Linheng Li at the Stowers Institute for Medical Research (Kansas City, MO) for providing the phospho- β -catenin antibody. This work was supported in part by National Institutes of Health Grants CA121105 (to L.Z.), CA106348 (to L.Z.), CA129829 (to J.Y.), and U01-DK085570 (to J.Y.), the latter as part of the Intestinal Stem Cell Consortium, a collaborative research project funded by the National Institute of Diabetes and Digestive and Kidney Diseases. This work was also supported by American Cancer Society Grants R5G-07-156-01-CNE (to L.Z.) and RGS-10-124-01-CCE (to J.Y.) and a grant from the Flight Attendant Medical Research Institute (to J.Y.).

1. Hong WK, Sporn MB (1997) Recent advances in chemoprevention of cancer. *Science* 278:1073–1077.
2. Stoner GD (2009) Foodstuffs for preventing cancer: The preclinical and clinical development of berries. *Cancer Prev Res (Phila)* 2:187–194.
3. Thun MJ, Henley SJ, Patrono C (2002) Nonsteroidal anti-inflammatory drugs as anticancer agents: Mechanistic, pharmacologic, and clinical issues. *J Natl Cancer Inst* 94:252–266.
4. Rao CV, Reddy BS (2004) NSAIDs and chemoprevention. *Curr Cancer Drug Targets* 4: 29–42.
5. Vogelstein B, Kinzler KW (2004) Cancer genes and the pathways they control. *Nat Med* 10:789–799.
6. Su LK, et al. (1992) Multiple intestinal neoplasia caused by a mutation in the murine homolog of the APC gene. *Science* 256:668–670.
7. Barker N, et al. (2009) Crypt stem cells as the cells-of-origin of intestinal cancer. *Nature* 457:608–611.
8. Sangiorgi E, Capocchi MR (2008) Bmi1 is expressed in vivo in intestinal stem cells. *Nat Genet* 40:915–920.
9. Li L, Clevers H (2010) Coexistence of quiescent and active adult stem cells in mammals. *Science* 327:542–545.
10. Barker N, et al. (2007) Identification of stem cells in small intestine and colon by marker gene Lgr5. *Nature* 449:1003–1007.
11. van der Flier LG, Haegbarth A, Stange DE, van de Wetering M, Clevers H (2009) OLFM4 is a robust marker for stem cells in human intestine and marks a subset of colorectal cancer cells. *Gastroenterology* 137:15–17.
12. Yu J, Zhang L (2004) Apoptosis in human cancer cells. *Curr Opin Oncol* 16:19–24.
13. Sun SY, Hail N, Jr., Lotan R (2004) Apoptosis as a novel target for cancer chemoprevention. *J Natl Cancer Inst* 96:662–672.
14. Zhang L, Yu J, Park BH, Kinzler KW, Vogelstein B (2000) Role of BAX in the apoptotic response to anticancer agents. *Science* 290:989–992.
15. Du C, Fang M, Li Y, Li L, Wang X (2000) Smac, a mitochondrial protein that promotes cytochrome c-dependent caspase activation by eliminating IAP inhibition. *Cell* 102: 33–42.
16. Bank A, Wang P, Du C, Yu J, Zhang L (2008) SMAC mimetics sensitize nonsteroidal anti-inflammatory drug-induced apoptosis by promoting caspase-3-mediated cytochrome c release. *Cancer Res* 68:276–284.
17. Kohli M, et al. (2004) SMAC/Diablo-dependent apoptosis induced by nonsteroidal antiinflammatory drugs (NSAIDs) in colon cancer cells. *Proc Natl Acad Sci USA* 101: 16897–16902.
18. Beazer-Barclay Y, et al. (1996) Sulindac suppresses tumorigenesis in the Min mouse. *Carcinogenesis* 17:1757–1760.
19. McEntee MF, Chiu CH, Whelan J (1999) Relationship of beta-catenin and Bcl-2 expression to sulindac-induced regression of intestinal tumors in Min mice. *Carcinogenesis* 20:635–640.
20. Corpet DE, Pierre F (2003) Point: From animal models to prevention of colon cancer. Systematic review of chemoprevention in min mice and choice of the model system. *Cancer Epidemiol Biomarkers Prev* 12:391–400.
21. Qiu W, et al. (2008) PUMA regulates intestinal progenitor cell radiosensitivity and gastrointestinal syndrome. *Cell Stem Cell* 2:576–583.
22. Shoemaker AR, Gould KA, Luongo C, Moser AR, Dove WF (1997) Studies of neoplasia in the Min mouse. *Biochim Biophys Acta* 1332:F25–F48.
23. Clevers H (2006) Wnt/beta-catenin signaling in development and disease. *Cell* 127: 469–480.
24. He XC, et al. (2007) PTEN-deficient intestinal stem cells initiate intestinal polyposis. *Nat Genet* 39:189–198.
25. Oue N, et al. (2009) Serum olfactomedin 4 (GW112, hGC-1) in combination with Reg IV is a highly sensitive biomarker for gastric cancer patients. *Int J Cancer* 125: 2383–2392.
26. Rosen JM, Jordan CT (2009) The increasing complexity of the cancer stem cell paradigm. *Science* 324:1670–1673.
27. Yu J (2009) PUMA kills stem cells to stall cancer? *Mol Cell Pharmacol (Windsor Mill)* 1: 112–118.
28. Hall PA, Coates PJ, Ansari B, Hopwood D (1994) Regulation of cell number in the mammalian gastrointestinal tract: The importance of apoptosis. *J Cell Sci* 107: 3569–3577.
29. Keller JJ, Giardiello FM (2003) Chemoprevention strategies using NSAIDs and COX-2 inhibitors. *Cancer Biol Ther* 2(suppl 1):S140–S149.
30. Deng Y, Ren X, Yang L, Lin Y, Wu X (2003) A JNK-dependent pathway is required for TNFalpha-induced apoptosis. *Cell* 115:61–70.
31. Zhang L, et al. (2010) Chemoprevention of colorectal cancer by targeting APC-deficient cells for apoptosis. *Nature* 464:1058–1061.
32. Yu J, et al. (2007) Induced pluripotent stem cell lines derived from human somatic cells. *Science* 318:1917–1920.
33. Hermeking H, Eick D (1994) Mediation of c-Myc-induced apoptosis by p53. *Science* 265:2091–2093.
34. Meyskens FL, Jr., et al. (2008) Difluoromethylornithine plus sulindac for the prevention of sporadic colorectal adenomas: A randomized placebo-controlled, double-blind trial. *Cancer Prev Res (Phila)* 1:32–38.
35. Okada H, et al. (2002) Generation and characterization of Smac/DIABLO-deficient mice. *Mol Cell Biol* 22:3509–3517.
36. Qiu W, Carson-Walter EB, Kuan SF, Zhang L, Yu J (2009) PUMA suppresses intestinal tumorigenesis in mice. *Cancer Res* 69:4999–5006.
37. Qiu W, Leibowitz B, Zhang L, Yu J (2010) Growth factors protect intestinal stem cells from radiation-induced apoptosis by suppressing PUMA through the PI3K/AKT/p53 axis. *Oncogene* 29:1622–1632.



Cancer Research

CDX2 Regulates *Multidrug Resistance 1* Gene Expression in Malignant Intestinal Epithelium

Yuji Takakura, Takao Hinoi, Naohide Oue, et al.

Cancer Res 2010;70:6767-6778. Published OnlineFirst August 10, 2010.

Updated Version

Access the most recent version of this article at:
[doi:10.1158/0008-5472.CAN-09-4701](https://doi.org/10.1158/0008-5472.CAN-09-4701)

Supplementary Material

Access the most recent supplemental material at:
<http://cancerres.aacrjournals.org/content/suppl/2010/08/09/0008-5472.CAN-09-4701.DC1.html>

Cited Articles

This article cites 46 articles, 24 of which you can access for free at:
<http://cancerres.aacrjournals.org/content/70/17/6767.full.html#ref-list-1>

E-mail alerts

Sign up to receive free email-alerts related to this article or journal.

Reprints and Subscriptions

To order reprints of this article or to subscribe to the journal, contact the AACR Publications Department at pubs@aacr.org.

Permissions

To request permission to re-use all or part of this article, contact the AACR Publications Department at permissions@aacr.org.

Molecular and Cellular Pathobiology

CDX2 Regulates *Multidrug Resistance 1* Gene Expression in Malignant Intestinal EpitheliumYuji Takakura¹, Takao Hinoi², Naohide Oue³, Tatsunari Sasada¹, Yasuo Kawaguchi¹, Masazumi Okajima², Aytekin Akyol⁴, Eric R. Fearon⁴, Wataru Yasui³, and Hideki Ohdan¹

Abstract

The caudal-related homeobox transcription factor CDX2 has a key role in intestinal development and differentiation. *CDX2* heterozygous mutant mice develop colonic polyps, and loss of CDX2 expression is seen in a subset of colon carcinomas in humans. Ectopic CDX2 expression in the stomach of transgenic mice promotes intestinal metaplasia, and CDX2 expression is frequently detected in intestinal metaplasia in the stomach and esophagus. We sought to define CDX2-regulated genes to enhance knowledge of CDX2 function. HT-29 colorectal cancer cells have minimal endogenous CDX2 expression, and HT-29 cells with ectopic CDX2 expression were generated. Microarray-based gene expression studies revealed that the *Multidrug Resistance 1* (*MDR1/P-glycoprotein/ABCBI*) gene was activated by CDX2. Evidence that the *MDR1* gene was a direct transcriptional target of CDX2 was obtained, including analyses with *MDR1* reporter gene constructs and chromatin immunoprecipitation assays. RNA interference-mediated inhibition of CDX2 decreased endogenous *MDR1* expression. In various colorectal cancer cell lines and human tissues, endogenous *MDR1* expression was well correlated to CDX2 expression. Overexpression of CDX2 in HT-29 cells revealed increased resistance to the known substrate of *MDR1*, vincristine and paclitaxel, which was reversed by an *MDR1* inhibitor, verapamil. These data indicate that CDX2 directly regulates *MDR1* gene expression through binding to elements in the promoter region. Thus, CDX2 is probably important for basal expression of *MDR1*, regulating drug excretion and absorption in the lower gastrointestinal tract, as well as for multidrug resistance to chemotherapy reagent in CDX2-positive gastrointestinal cancers. *Cancer Res*; 70(17): 6767-78. ©2010 AACR.

Introduction

There has long been great interest in defining critical regulatory factors that direct cell fate determination and differentiation in normal and cancer tissues. In mammals, the CDX1 and CDX2 homeobox transcription factors apparently have critical functions in intestinal development, differentiation, and maintenance of the intestinal phenotype (1, 2). CDX1 and CDX2 proteins show significant homology, particularly in their homeobox DNA-binding domains, to the protein product of the *Drosophila caudal gene*, a key regulator of

anterior-posterior regional identity (1, 3, 4). Mouse *Cdx1* and *Cdx2* genes are quite broadly expressed during early embryonic development. Recent studies indicated that *Cdx2* is one of the earliest transcription factors essential for formation and maintenance of the trophoblast lineage in mouse embryos (5, 6). However, in later stages of development and in normal adult tissues, expression of the genes is apparently restricted to epithelium of the small intestine and colon (1). In support of the view that CDX proteins play key roles in regulating proliferation and intestinal cell fate, mice with constitutional inactivating mutations in one *Cdx2* allele (*Cdx2±*) developed multiple polyps in the proximal colon (7-10). The epithelial cells in these polyps often lose intestinal differentiation features, displaying areas of stratified squamous epithelium similar to that in forestomach and distal esophagus as well as areas resembling normal gastric mucosa (7, 11). Ectopic expression of *Cdx2* in the gastric mucosa of transgenic mice was reported to induce intestinal metaplasia (12, 13). In humans, loss of the *CDX1* and/or *CDX2* gene and protein expression was observed in a subset of primary colorectal cancers (CRC) and cancer cell lines (14), usually in poorly differentiated CRCs (15). Aberrant (ectopic) expression of CDX2 is detected frequently in intestinal metaplasia of the stomach (16, 17).

Our prior efforts to identify CDX2-regulated genes indicated that liver intestine-cadherin (LI-cadherin) and hephaestin

Authors' Affiliations: Departments of ¹Surgery, ²Endoscopic Surgery and Surgical Science, and ³Molecular Pathology, Division of Frontier Medical Science, Programs for Biomedical Research, Graduate School of Biomedical Science, Hiroshima University, Hiroshima, Japan; and ⁴Division of Molecular Medicine and Genetics, Departments of Internal Medicine, Human Genetics, and Pathology, University of Michigan Medical School, Ann Arbor, Michigan

Note: Supplementary data for this article are available at Cancer Research Online (<http://cancerres.aacrjournals.org/>).

Present address for A. Akyol: Hacettepe University School of Medicine, Department of Pathology, Ankara, Turkey.

Corresponding Author: Takao Hinoi, Department of Endoscopic Surgery and Surgical Science, Hiroshima University, 1-2-3 Kasumi, Minami-ku, Hiroshima, 734-8551, Japan. Phone: 81-82-257-5222; Fax: 81-82-257-5224; E-mail: thinoi@hiroshima-u.ac.jp.

doi: 10.1158/0008-5472.CAN-09-4701

©2010 American Association for Cancer Research.

(HEPH) were likely key molecules regulated by CDX2 in normal and malignant gastrointestinal epithelium (16, 18).

Here, we report on further studies to implicate CDX2 in regulating the expression of intestinal-specific genes by using high-density oligonucleotide microarrays as a starting point to identify potential CDX2-regulated genes in HT-29, a CRC cell line with significantly decreased endogenous CDX2 expression. In HT-29 cell line engineered to express CDX2 ectopically, the gene for *Multidrug Resistance 1* (*MDR1*) was strongly activated.

Of some potential interest, *MDR1* was originally identified as an overexpressed and amplified gene in multiple drug-resistant cells, and its product, P-glycoprotein, seems to play a critical role in drug resistance (19). We provide data here implicating CDX2 as an important factor in regulation of *MDR1* expression in gastrointestinal tissues.

Materials and Methods

Plasmids

A full-length, wild-type *CDX2* and *CDX1* allele were amplified by PCR using hexamer-primed complementary DNA (cDNA) from normal human colon tissue as a template. Sequence coding Flag epitope was added to the 5' ends of *CDX1* allele. The *CDX2* and Flag-*CDX1* allele were inserted into the multiple cloning site of the retroviral expression vector pPGS-CMV-CITE-neo (pPGS-neo, provided by G. Nabal, NIH, Bethesda, MD) to generate pPGS-CDX2. The full-length, wild-type *CDX2* allele was also subcloned into the retroviral vector pBabe-Puro ER (provided by A. Friedman, Johns Hopkins Oncology Center, Baltimore, MD; ref. 20) to generate pCDX2-ER. The pCDX2-ER vector encodes a chimeric protein in which full-length CDX2 sequences are fused upstream of a mutated estrogen receptor (ER) ligand-binding domain. The mutated ER ligand-binding domain no longer binds estrogen, but retains the ability to bind tamoxifen. Fragments from human *MDR1* and *glyceraldehyde-3-phosphate dehydrogenase* (*GAPDH*) genes were generated by PCR using hexamer-primed cDNA from Caco2 cells as a template (16). A 309-bp fragment of *MDR1* cDNA was amplified using forward primer 5'-CAGTGAAGTCTGACTCTATGAGATG-3' and reverse primer 5'-AGCAAGGCAGTCAGTTACAGTCC-3'. The *MDR1* and *GAPDH* cDNA fragments were subcloned into the pGEM-T Easy Vector (Promega). Genomic DNA sequences from the promoter regions of the human *MDR1* gene were cloned by PCR, using genomic DNA purified from DLD-1 cells as a template, with the reverse primer 5'-GGCTCGAG-GAAACAGGTTGAATTTCCAGG-3' and the following forward primers: 5'-GCGGGTACCAGGCATTTAGCCTACTAGTG-3' (from -4,003), 5'-ATGGTACCACATGTGAAAGG-GTGGAGAGTG-3' (from -3,414), 5'-CCGGTACC-ATGTCAGTGGAGCAAAGAAATG-3' (from -1,711), and 5'-CCGGTACCGTGAAACAATGCTGTACACTTGC-3' (from -1,422). The PCR products were digested with KpnI and XhoI (sites underlined in the primers) and subcloned into pGL4.10 [*luc2*] vector (Promega). PCR-based approaches were used to introduce mutations into the presumptive CDX2-binding sites in the pGL4.10-MDR1 (-4,203/+50)

reporter gene construct. Sequence of presumptive CDX2 binding site A (ATTTATG) and B (TTTTATG) were changed to ACCTGCG and TCCTGCG in the primer using the primers: 5'-GCGGTACCAGGCATTTAGCCTACTAGTGTAATTTCC-GCAGGTC-3' and 5'-GAGCGGGCTTCTCAGATGATATGTGCTTTTCACTCTGTGC-3' (for binding site A), and 5'-GCGGGTACCAGGCATTTAGCCTACTAGTG-3', 5'-GCATGTCCTTCATACGCAGGAATCATTACATGTG-3', 5'-GCGTATGAAGGACATGTGATGATAGGGG-3', and 5'-GGGCTTCTCAGATGATATGTGCTTTTCACTC-3' (for binding site B). All fragments generated by PCR were verified by automated sequencing of the respective plasmid constructs. Plasmid pGL4.74 [*hRluc*/TK] vector (Promega) was used as control for transfection efficiency in reporter assays.

Cell culture and retrovirus infections

The amphotropic Phoenix packaging cell line was provided by G. Nolan (Stanford University, Stanford, CA). All other cell lines were obtained from the American Type Culture Collection in 1998 to 2000. Frozen stock was made immediately and stored in liquid nitrogen until the initiation of this study. After thawing frozen stock, the cells were kept at low passage throughout the study. The cell morphology was monitored by microscopy and confirmed that their morphologic images were maintained in comparison with the original morphologic images. Details of cell culture conditions were previously described (16). The Phoenix packaging cells were transfected with retroviral expression constructs (pPGS-CDX2, pPGS-neo, pPGS-Flag-CDX1, and pCDX2-ER); the supernatant containing nonreplicating amphotropic virus was harvested as previously described (16). HT-29 cells were infected with virus, selected, and maintained in media containing G418 (Invitrogen) or Puromycin (Sigma). In HT-29 cells expressing the CDX2-ER fusion protein (HT-29/CDX2-ER), CDX2 function was activated by addition of 4-hydroxytamoxifen (4-OHT; Sigma) to the growth medium at a final concentration of 500 nmol/L. To assess *MDR1* as a direct CDX2-regulated target gene, HT-29/CDX2-ER cells were treated with the protein synthesis inhibitor cycloheximide (Sigma) at a concentration of 1 μ g/mL.

Complementary RNA synthesis and gene expression profiling

Total RNA was prepared by Trizol (Invitrogen) extraction and purification with the RNeasy Cleanup kit (Qiagen). Gene expression analyses were performed with GeneChip Human Genome U95Av2 and U133A (Affymetrix, Inc.) following supplier instructions. Affymetrix arrays were scanned using the GeneArray scanner (Affymetrix); image analysis was performed with the GeneChip 4.0 software (Affymetrix).

Northern blot analysis

For each sample, 10 μ g of total RNA were fractionated by electrophoresis and transferred to a Zeta-Probe GT membrane (Bio-Rad Laboratories). Hybridization was performed using 32 P-radiolabeled cloned cDNA fragments of *MDR1*, as previously described (16). The membrane was stripped and reprobed with *GAPDH* cDNA to confirm equivalent loading and RNA transfer.

Western blot assays

Western blot analysis was performed essentially as previously described (16). Anti-CDX2 mouse monoclonal antibodies (clone 7C7/D4, BioGenex Laboratories, Inc.), antihuman MDR1 monoclonal antibody (clone C219, Calbiochem), and anti-Flag M2 monoclonal antibody (Sigma) were used at 1:10,000, 1:50, and 1:500 dilutions, respectively. The membrane was stripped and reprobed with an anti- β -actin monoclonal antibody (clone AC-15; Sigma) to verify loading and transfer.

RNA interference

Two small interfering RNA (siRNA) duplexes targeting CDX2 (5'-AACCAGGACGAAAGACAAAUA-3', CDX2 siRNA-1; and 5'-AAGCCUCAGUGUCUGGCUCUG-3', CDX2 siRNA-2) and a nonsilencing siRNA duplex (5'-AAUUCUCCGAACGUGACAGU-3') were synthesized by Qiagen-Xeragon. Cells were cultured in antibiotic-free medium for 24 hours before transfection. They were then transfected with siRNA (340 pmol) using DharmaFECT1 (Dharmacon). Silencing was examined 72 hours after transfection. Each sample was reverse transcribed using the ReverTra Ace qPCR RT kit (Toyobo) following supplier protocols. Quantitative PCR (qPCR) analysis was performed on an ABI 7500HT with Power SYBR Green PCR Master Mix (Applied Biosystems). *MDR1* primers were as follows: forward, 5'-ATAATGCGACAGGAGATAGG-3'; and reverse, 5'-CCAAAATCACAAGGGTTAGC-3'. *GAPDH* primers were as follows: forward, 5'-TTGAGGTCAATGAAGGGG-3'; and reverse, 5'-GAAGGTGAAGGTCCGAGTC-3'. All experiments were conducted three times. Human *GAPDH* was measured as the internal control.

Reporter gene assays

At 48 hours before transfection, cells were seeded in 35-mm dishes. HT29/PGS-CDX2 and HT29/PGS-neo cells were transfected at 50% to 80% confluency with 4 μ L of Lipofectamine 2000 (Invitrogen), 0.5 μ g of pGL4.10 reporter gene construct, and 0.05 μ g of control plasmid pGL4.74. At 40 hours after transfection, cells were collected and resuspended in passive lysis buffer (Promega). Luciferase activity was determined with a dual luciferase assay system (GloMax96 Microplate Luminometer, Promega).

Chromatin immunoprecipitation assay

The chromatin immunoprecipitation (ChIP) assays were performed using the ChIP-IT Express kit (Active Motif) following supplier instructions. Chromatin extracts containing DNA fragments (average size, 500 bp) were immunoprecipitated using 2 μ g monoclonal anti-CDX2 antibody (7C7/D4) or 2 μ g nonimmunized mouse IgG whole molecule (negative control, Active Motif). Fragments (200 bp) of the *MDR1* promoter regions were PCR amplified using the primers 5'-CCTGGGAGACAGAGTAATAC-3' (forward) and 5'-CAAAGTGGACAGAGACTTATAC-3' (reverse; -4,100/-3,882, including binding site A), and 5'-ATCCCTATCAAGTACAGTC-3' (forward) and 5'-CTCAGTCCAAAGAGCAAGAC-3' (reverse; -3,482/-3,296, including binding site B). As a negative control, a 4-kb DNA fragment from exon 3 of the *CDX1* gene was amplified by PCR using previously described

primers (18). Each immunoprecipitated DNA sample was quantified using the average of duplicate qPCRs. All ChIP-qPCR signals were normalized to the input (labeled as IP/input). Each primer gave a single product of the right size, as confirmed by agarose gel electrophoresis.

Immunohistochemical staining

Formalin-fixed, paraffin-embedded tissues were stained using the avidin-biotin complex method as previously described (16). Mouse monoclonal anti-CDX2 antibody 7C7/D4 and mouse monoclonal anti-MDR1 antibody (clone C494; Zymed Laboratories) were used at 1:1,000 and 1:10 dilution, respectively.

Cytotoxicity assay

Paclitaxel and verapamil were purchased from Sigma, and 5-fluorouracil was provided by Kyowa Hakko Kogyo Co. Ltd. Doxorubicin and vincristine were provided by Nippon Kayaku. Camptothecin and cisplatin were purchased from LKT Laboratories. MTT cytotoxicity assay was used to examine cell survival after exposure to chemotherapeutic agents. Cells were seeded at 5,000 cells/100 μ L per well in 96-well microtiter plates. After a 48-hour incubation period, cells were treated with a range of concentrations of each chemotherapeutic agent. To examine the effect of verapamil, a known P-glycoprotein inhibitor (21), 2 μ mol/L were administered together with each chemotherapeutic agent. A pilot experiment showed that this concentration was not cytotoxic to HT-29/PGS-CDX2 or HT-29/PGS-neo cells (data not shown). After 72 hours, 10 μ L of MTT dye (5 mg/mL) was added to each well, and plates were incubated for 4 hours at 37°C in a humidified 5% CO₂ atmosphere. Dark blue formazan crystals formed by live cells were dissolved in 100 μ L of solubilization solution (10% SDS in 0.01 mol/L HCl). Absorbance in individual wells was determined at 570 nm using an MTP-300 microplate reader (CORONA Electric Co. Ltd.). Results were expressed in terms of the concentration required to inhibit cell growth by 50% relative to nontreated cells [IC₅₀ (72 h)].

Results

CDX2 and MDR1 expression are correlated in colon carcinoma cells

Similar to a few selected other human CRC cell lines, the HT-29 line shows very low endogenous CDX2 expression (22). To identify candidate CDX2-regulated genes, we generated polyclonal populations of HT-29 CRC cells ectopically expressing CDX2, by infecting the cells with replication-defective retroviruses carrying full-length human *CDX2* cDNA (Fig. 1A). Comparison of gene expression in the HT-29/PGS-CDX2 cells versus control populations (HT-29/PGS-neo) was performed using microarrays with focus on the *MDR1* (*ABCB1*) gene. Affymetrix data indicated that *MDR1* gene expression was upregulated by CDX2 by roughly 31.14-fold in HT-29 cells (Fig. 1A). Northern and Western blot studies confirmed robust induction of *MDR1* transcripts and protein in HT-29/PGS-CDX2 cells (Fig. 1B). To determine whether MDR1 is a selective CDX2 target, we also generated polyclonal

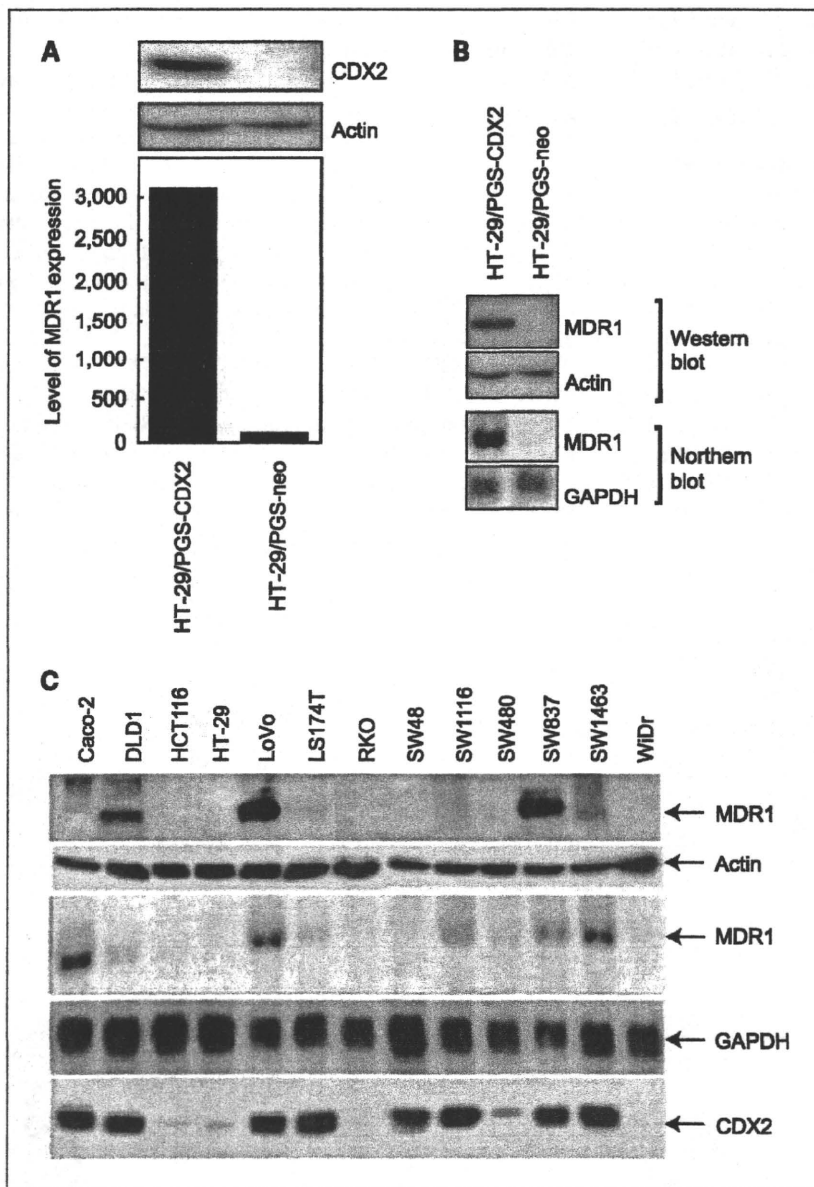


Figure 1. CDX2 activates *MDR1* expression in HT-29 cells. **A**, top, a monoclonal anti-CDX2 antibody detects the roughly 40-kDa CDX2 protein in HT-29/PGS-CDX2 cells but not in HT-29/PGS-neo cells. **A**, bottom, relative level of *MDR1* gene expression in HT-29/PGS-CDX2 and HT-29/PGS-neo in Affymetrix microarray studies. **B**, Northern and Western blot analysis detects *MDR1* transcripts and products in HT-29/PGS-CDX2 with low or absent *MDR1* expression in HT-29/PGS-neo cells. In Western blot analysis, a mouse monoclonal anti-*MDR1* antibody detects the roughly 170-kDa *MDR1* product in HT-29/PGS-CDX2 cells but not in HT-29/PGS-neo cells. **C**, expression of CDX2 and *MDR1* in 13 CRC cell lines. In the indicated 13 CRC cell lines, Western blot analyses of *MDR1* and CDX2 expression were performed using a mouse monoclonal antibody against human *MDR1* and a mouse monoclonal antibody against human CDX2. The membranes were stripped and reprobbed with a monoclonal antibody against β -actin to verify loading and transfer. Northern blot analysis of *MDR1* expression was performed using an *MDR1* cDNA probe. The membrane was stripped and reprobbed with a GAPDH cDNA probe to verify loading and transfer.

populations of HT-29 cells ectopically expressing CDX1 (HT-29/PGS-Flag-CDX1). In this cell line, *MDR1* expression was not induced by overexpression of CDX1 (Supplementary Fig. S1).

To assess the correlation between endogenous *CDX2* and *MDR1* expression in other CRC cell lines, Northern and Western blot analyses were performed on 12 additional lines. *MDR1* protein expression was detected in six cell lines with high levels of *MDR1* transcripts. In all of these cell lines, strong CDX2 expression was observed (Fig. 1C, lanes 1, 2, 5, 9, 11, and 12, 5, 9, 11, and 12). However, none of the cell lines with weak or undetectable CDX2 expression had detectable *MDR1* transcripts or protein.

The *MDR1* gene is a primary target of CDX2 activity

To better assess the relationship between CDX2 function and *MDR1* gene expression, we studied *MDR1* expression in

an HT-29-derived line with tightly regulated CDX2 activity. We used a polyclonal HT-29 cell line that had been transduced with a vector encoding a chimeric CDX2-ER fusion protein. In the chimeric CDX2-ER protein, full-length CDX2 sequences are present upstream of a mutated ER ligand-binding domain. The mutant ER ligand-binding domain is capable of binding to 4-OHT, but not estrogen. Expression of the CDX2-ER fusion protein in HT-29/CDX2-ER polyclonal cell line was confirmed (data not shown). Treatment of HT-29/CDX2-ER cell line with 4-OHT strongly induced *MDR1* expression within 12 hours, with further increased expression up to day 2 of 4-OHT treatment (Fig. 2A). Consistent with the notion that *MDR1* is a direct or primary target gene regulated by CDX2, blockade of new protein synthesis by cycloheximide treatment did not inhibit induction of *MDR1*